IN-66
140760
P.34

NASA Contractor Report 189740
ICASE Report No. 92–66

ICASE

THE MODELING OF PIEZOCERAMIC PATCH INTERACTIONS WITH SHELLS, PLATES AND BEAMS

(NASA-CR-189740) THE MODELING OF PIEZOCERAMIC PATCH INTERACTIONS WITH SHELLS, PLATES AND BEAMS Final Report (ICASE) 34 p
N93-16611
Unclas
G3/66 0140760

H. T. Banks
R. C. Smith

NASA Contract Nos. NAS1–18605 and NAS1–19480
December 1992

Institute for Computer Applications in Science and Engineering
NASA Langley Research Center
Hampton, Virginia 23681–0001

Operated by the Universities Space Research Association

National Aeronautics and
Space Administration

Langley Research Center
Hampton, Virginia 23665-5225

THE MODELING OF PIEZOCERAMIC PATCH INTERACTIONS WITH SHELLS, PLATES AND BEAMS [1]

H.T. Banks
Center for Research in Scientific Computation
North Carolina State University
Raleigh, NC 27695

R.C. Smith
ICASE
NASA Langley Research Center
Hampton, VA 23681

ABSTRACT

General models describing the interactions between a pair of piezoceramic patches and elastic substructures consisting of a cylindrical shell, plate and beam are presented. In each case, the manner in which the patch loads enter both the strong and weak forms of the time-dependent structural equations of motion is described. Through force and moment balancing, these loads are then determined in terms of material properties of the patch and substructure (thickness, elastic properties, Poisson ratios), the geometry of the patch placement, and the voltages into the patches. In the case of the shell, the coupling between bending and in-plane deformations, which is due to the curvature, is retained. These models are sufficiently general to allow for potentially different patch voltages which implies that they can be suitably employed when using piezoceramic patches for controlling system dynamics when both extensional and bending vibrations are present.

[1]The research of H.T.B. was supported in part by the Air Force Office of Scientific Research under grant AFOSR-90-0091. This research was also supported by the National Aeronautics and Space Administration under NASA Contract Numbers NAS1-18605 and NAS1-19480 while H.T.B. was a visiting scientist and R.C.S. was in residence at the Institute for Computer Applications in Science and Engineering (ICASE), NASA Langley Research Center, Hampton, VA 23681. Finally, the work of H.T.B. was completed in part while the author was a visitor at the Institute for Mathematics and Its Applications, University of Minnesota, Minneapolis, MN 55455.

1 Introduction

The use of piezoceramic elements as sensors and actuators has burgeoned in the last several years in applications ranging from the measurement and damping of vibrations in large flexible structures to the control of noise in structural acoustics settings. Their utility as sensors derives from the property that when the element is subjected to a mechanical strain, a voltage proportional to the strain is produced. Conversely, they also exhibit the phenomenon that an applied polarization voltage across the unconstrained element produces in-plane mechanical strains in the material. Because of these properties, piezoceramic elements have found increasing success both as sensors such as strain gauges and accelerometers and as distributed actuators. Their success as actuators is augmented by the fact that they can be used to directly control local vibrations without applying rigid body forces and torques, and due to their distributed nature, they are less prone to spillover effects in many control strategies. Moreover, the piezoceramic elements or patches are inexpensive, lightweight, space efficient and can be easily shaped or bonded to a variety of surfaces. Hence a large number of patches can be used to sense and control without significantly changing the mass or dynamic properties of the system.

In order to obtain optimal results with the piezoceramic elements or patches in sensing and control applications, it is necessary to have accurate models of the mechanics of induced strain actuation. This modeling also provides knowledge of the physical limitations of the piezoceramic patches as actuators in various settings. Detailed models have been developed for piezoceramic patch interaction with Euler-Bernoulli beams [2, 3, 4, 5, 10] and thin plates [6, 12]. Because many of the initial applications of piezoceramic elements were in settings involving the sensing and control of bending deformations (these vibrations are dominant in many low frequency vibration and noise control problems), most of these models concentrate on patch configurations which excite pure bending motion of the substructure with more limited discussions of pure extensional excitation. It was not until [10] that a model was developed which provided for simultaneous excitation of both bending and extensional deformations in an Euler-Bernoulli beam. One motivation for developing such a model is the observation that in complex coupled systems, in-plane vibrations with small displacements can have large in-plane energy levels due to the property that beams are much stiffer in extension than in bending. This in-plane energy can then couple into flexural vibrations at structural discontinuities such as joints, thus necessitating the control of both bending and extensional vibrations in such structures. As determined by Fuller et al [8] through experimental work, simultaneous reductions in both flexural and extensional deformations in a beam can be obtained through the use of asymmetric pairs of piezoceramic actuators and sensors in adaptive control schemes, and the analytic work in [10] was a first step toward developing a model which could be used in further such control settings. In that work, force and moment balancing were used to determine expressions for the moments and strains induced by the activation of a single piezoceramic patch which was bonded to an Euler-Bernoulli beam.

In addition to beams and plates, thin elastic shells are often used to describe various structural components as well as when modeling the coupling between structural vibrations and their radiating or receiving acoustic fields. For example, the transmission of sound through an airplane fuselage due to low frequency, high amplitude exterior acoustic fields can be modeled by a vibrating thin cylindrical shell which is coupled to an interior acoustic pressure field [9]. In order to optimally control the interior noise via piezoceramic patch actuation, one first needs to accurately model the interactions between the patches and the shell. This raises modeling issues which differ from those encountered in the beam and plate analyses in that the in-plane and bending vibrations are coupled in the cylindrical shell due to curvature effects.

Analytical models describing piezoceramic patch/cylindrical shell interactions have primarily been based on layered shell theory [11, 19] or the use of flat plate piezoceramic coupling results when determining the resulting loading on the shell [15]. In the first case it is assumed that the piezoceramic material makes up an entire layer of the elastic structure and hence this model is of limited use when considering small patches as actuators. When using the flat plate theory, it is assumed that the patch dimensions are small in comparison with the cylinder radius. Curvature properties are then neglected when modeling the coupling between the patch and shell and determining the loading due to activation of the patch.

In this work, we present general models for the interactions between a pair of piezoceramic patches and elastic substructures consisting of a beam, plate or thin shell. In the case of a shell, the patches are assumed to be curved and the coupling between bending and in-plane deformations, which is due to the curvature, is retained. The techniques used to develop the shell/patch interaction model are also used to develop general models describing the moments and forces which are generated by the activation of piezoceramic patches which have been bonded to a flat plate or beam. These models differ from those in [6, 12] and [2, 3, 4, 5] in that they allow for different voltages into the individual patches thus admitting the analysis of simultaneous excitations of both bending and extensional components. In the case of the beam, the model is slightly more general than that in [10] since it is derived for two active patches. Hence it is appropriate for models in which both patches actuate with potentially different voltages into the patches. In the case of one actuating patch, however, the model reduces to that in [10]. From a control perspective, these models are important since they provide for greater latitude in designing control strategies involving the use of piezoceramic elements to affect both the bending and extensional properties of a structure.

As a prelude to the development of the patch interaction models, equations of motion for the underlying substructures are presented with special attention paid to the contributions due to externally applied moments and forces since this is where the interactions between the patches and substructure occur. The analysis leading up to the structural equations also motivates many of the techniques which are used to develop the patch interaction models.

To this end, a synopsis of the derivation of the strong form of the time-dependent Donnell-Mushtari thin shell equations from Newtonian principles (force and moment balancing) is presented in Section 2. A complete treatment of this topic can be found in [13, 14, 16, 17, 18] and the included discussion is limited to summarizing that material which is needed for developing the shell/patch interaction model as presented in the following section. The choice of the Donnell-Mushtari model is for ease of presentation and as noted at various points in the discussion, the patch/shell interaction model can be easily extended to higher order models

as warranted by the physical situation.

An inherent disadvantage of the strong form for the equilibrium equations when the external loads are generated by piezoceramic elements is the resulting presence of the first and second derivatives of the Heaviside function due to the finite support of the patches. As a result of this as well as other identification and approximation issues, we then develop the weak form of the time-dependent Donnell-Mushtari shell equations. This is done in more detail since this development is less readily available in the the literature. This formulation is advantageous in many approximation schemes, admits the identification of discontinuous material parameters, and eliminates the problem of differentiating the Heaviside function since the derivatives are transferred onto the test functions.

The second section concludes with a synopsis of the strong and weak forms of the Kirchhoff plate and Euler-Bernoulli beam equations. As in the shell discussion, particular emphasis is placed on the contributions of externally applied forces and moments since this is where the coupling between the substructure and piezoceramic patches occurs.

The patch contributions to the cylindrical shell equations are developed in Section 3. In order to determine the loading due to patch moments and forces, it is useful to first express them in terms of the normal strains and changes in curvature of the middle surface of the cylindrical shell. To do this, the stress-strain relations in the patch and shell are developed which then allows the moment and force resultants for the patch to be formulated in terms of midsurface shell properties. The unknown normal strains and midsurface changes in curvature, and hence the patch moments and forces, are then determined by moment and force balancing. In this manner, the loading due to activation of the patches can be expressed in terms of material properties of the patches and shell (thickness, elastic properties, and Poisson ratios), the radius of curvature of the shell, and the voltage being applied to the patches.

In Section 4, the techniques of the third section are tailored to composite structures consisting of piezoceramic patches which are bonded to plates and beams. The resulting plate/patch interaction model is shown to be equivalent to that of [12] in the special case when pure bending motion is excited (the model in [12] was derived by isolating the interface stress for the system and treating it as the unknown to be determined). Due to its generality however, our model also allows for more complex interactions involving both bending and extensional components since the voltages into the individual patches can differ. As discussed earlier, the beam/patch interaction model reduces to the model in [10] in the case of one actuating patch but is slightly more general in that it also admits models in which two patches are used for actuating with potentially different voltages into the patches. As with the shells, this provides structure/patch interaction models which can be used in various structural and structural acoustics control settings.

2 Underlying Shell, Plate and Beam Equations

Throughout this discussion, we consider a thin circular cylindrical shell of radius R, thickness h and having the axial coordinate x as shown in Figure 1. The variable z measures the distance of a point on the shell from the corresponding point on the middle surface ($z = 0$) along the normal to the middle surface.

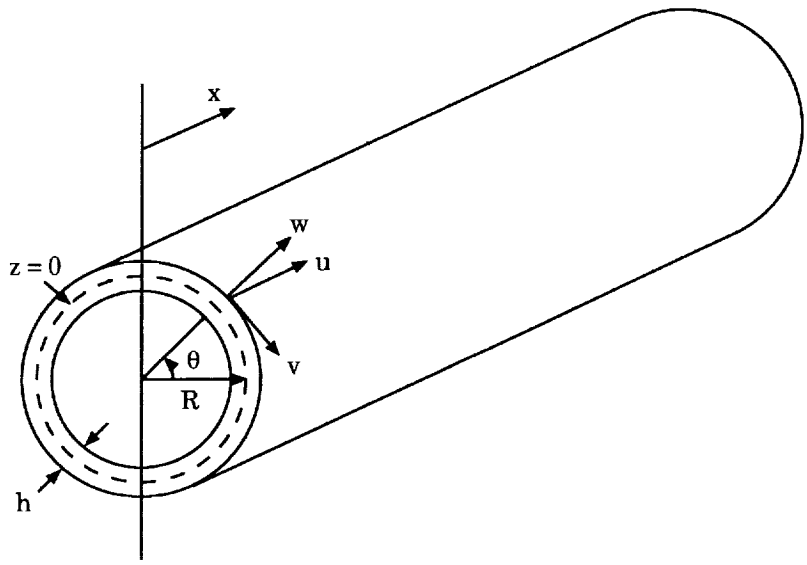

Figure 1. The Cylindrical Thin Shell.

Strain-Displacement Relations

By combining Love's shell assumptions with the strain-displacement equations of three dimensional elasticity theory, one obtains the strain relations

$$\begin{aligned} e_x &= \varepsilon_x + z\kappa_x \\ e_\theta &= \frac{1}{1 + \underline{z/R}} (\varepsilon_\theta + z\kappa_\theta) \\ \gamma_{x\theta} &= \frac{1}{1 + \underline{z/R}} \left[\varepsilon_{x\theta} + z\left(1 + \frac{z}{2R}\right)\tau\right] \end{aligned} \tag{2.1}$$

where e_x and e_θ are normal strains at an arbitrary point within the cylindrical shell and $\gamma_{x\theta}$ is the shear strain. Here ε_x, ε_θ and $\varepsilon_{x\theta}$ are the normal and shear strains in the middle surface and κ_x, κ_θ and τ are the midsurface changes in curvature and midsurface twist (see [14], page 8).

Note that within the framework of infinitesimal elasticity, the equations (2.1) are exact and in the Byrne-Flügge-Lur'ye shell theory, these represent the exact form of the kinematic

equations. In the Donnell-Mushtari theory, one neglects the underlined terms z/R with respect to unity thus leaving

$$\begin{aligned} e_x &= \varepsilon_x + z\kappa_x \\ e_\theta &= \varepsilon_\theta + z\kappa_\theta \\ \gamma_{x\theta} &= \varepsilon_{x\theta} + z\left(1 + \frac{z}{2R}\right)\tau \ . \end{aligned} \tag{2.2}$$

In terms of the axial, tangential and radial displacements u, v and w, respectively, the expressions for the midsurface strains and changes in curvature for the cylindrical shell are

$$\begin{aligned} \varepsilon_x &= \frac{\partial u}{\partial x} \qquad , \quad \kappa_x = -\frac{\partial^2 w}{\partial x^2} \\ \varepsilon_\theta &= \frac{1}{R}\frac{\partial v}{\partial \theta} + \frac{w}{R} \qquad , \quad \kappa_\theta = -\frac{1}{R^2}\frac{\partial^2 w}{\partial \theta^2} + \underline{\frac{1}{R^2}\frac{\partial v}{\partial \theta}} \\ \varepsilon_{x\theta} &= \frac{\partial v}{\partial x} + \frac{1}{R}\frac{\partial u}{\partial \theta} \qquad , \quad \tau = -\frac{2}{R}\frac{\partial^2 w}{\partial x \partial \theta} + \underline{\frac{2}{R}\frac{\partial v}{\partial x}} \ . \end{aligned} \tag{2.3}$$

As before, the underlined terms are retained in the Byrne, Flügge and Lur'ye theory and are discarded in the Donnell-Mushtari theory. We point out that the equations (2.1) and (2.3) differ from those arising in the theory of flat plates both in the presence of the length differential $Rd\theta$ as well as in the retention of the strain terms ε_x and ε_θ (only bending contributions are considered in the corresponding models of the transverse vibrations of a flat plate).

Stress-Strain Relations

To determine the constitutive properties of the shell, it is assumed that the shell material is elastic and isotropic. Hooke's law in conjunction with the assumption that the transverse shear stresses σ_{xz} and $\sigma_{\theta z}$ as well as the normal strain component e_z are small in comparison with other stresses and strains (these conditions are part of Love's third and fourth assumptions) then yields

$$\begin{aligned} \sigma_x &= \frac{E}{1-\nu^2}(e_x + \nu e_\theta) \\ \sigma_\theta &= \frac{E}{1-\nu^2}(e_\theta + \nu e_x) \\ \sigma_{x\theta} &= \sigma_{\theta x} = \frac{E}{2(1+\nu)}\gamma_{x\theta} \end{aligned} \tag{2.4}$$

where σ_x and σ_θ are normal stresses and $\sigma_{x\theta}$ and $\sigma_{\theta x}$ are tangential shear stresses. The constants E and ν are the Young's modulus and Poisson ratio for the shell.

Force and Moment Resultants

By integrating the stresses over the face of a fundamental element, the force resultants can be expressed as

$$\begin{bmatrix} N_x \\ N_{x\theta} \\ Q_x \end{bmatrix} = \int_{-h/2}^{h/2} \begin{bmatrix} \sigma_x \\ \sigma_{x\theta} \\ \sigma_{xz} \end{bmatrix} \left(1 + \frac{z}{R}\right) dz$$

and

$$\begin{bmatrix} N_\theta \\ N_{\theta x} \\ Q_\theta \end{bmatrix} = \int_{-h/2}^{h/2} \begin{bmatrix} \sigma_\theta \\ \sigma_{\theta x} \\ \sigma_{\theta z} \end{bmatrix} dz \ .$$

Similarly, the moment resultants are

$$\begin{bmatrix} M_x \\ M_{x\theta} \end{bmatrix} = \int_{-h/2}^{h/2} \begin{bmatrix} \sigma_x \\ \sigma_{x\theta} \end{bmatrix} \left(1 + \frac{z}{R}\right) z dz$$

and

$$\begin{bmatrix} M_\theta \\ M_{\theta x} \end{bmatrix} = \int_{-h/2}^{h/2} \begin{bmatrix} \sigma_\theta \\ \sigma_{\theta x} \end{bmatrix} z dz \ .$$

The orientation of the various forces and moments are shown in Figure 2. We point out that the transverse shear stresses σ_{xz} and $\sigma_{\theta z}$ are used when obtaining the force resultants Q_x and Q_θ even though they are omitted in the constitutive relations. This is one of the contradictions which arises in the classical shell theory.

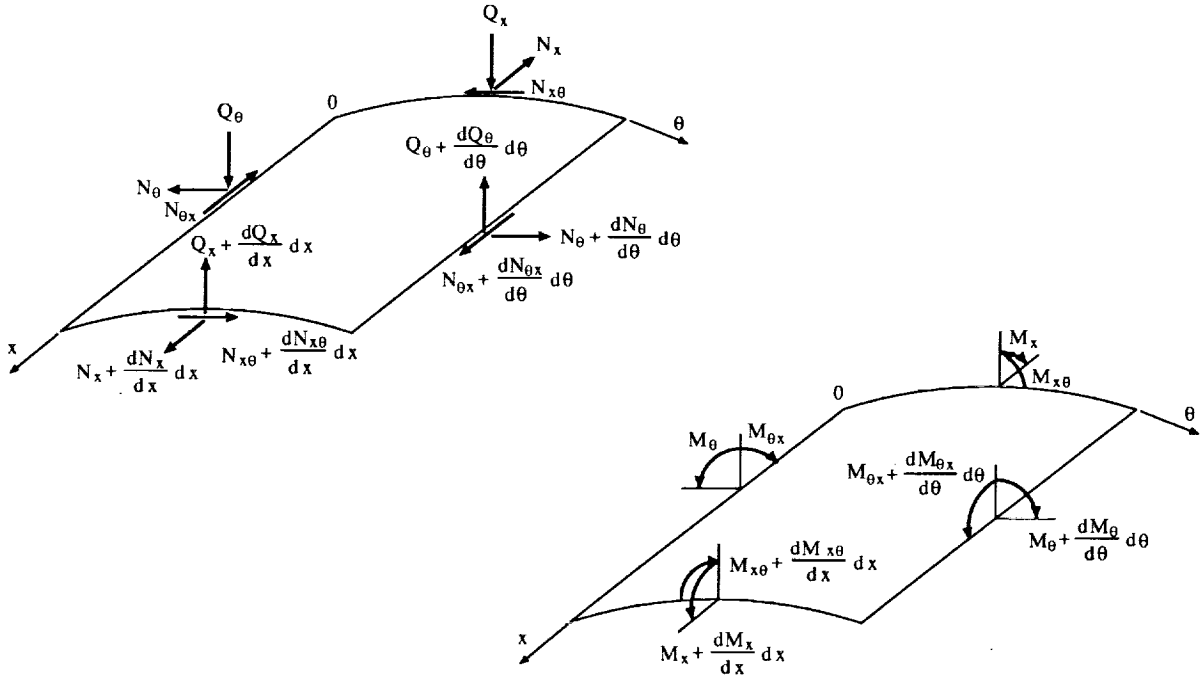

Figure 2. Force and Moment Resultants for the Cylindrical Shell.

In the Donnell-Mushtari theory, the underlined terms z/R are neglected in comparison to unity, and the integrals are determined accordingly to yield

$$
\begin{aligned}
N_x &= \frac{Eh}{(1-\nu^2)}\left[\frac{\partial u}{\partial x} + \nu\left(\frac{1}{R}\frac{\partial v}{\partial \theta} + \frac{w}{R}\right)\right] \quad , \quad M_x = -\frac{Eh^3}{12(1-\nu^2)}\left[\frac{\partial^2 w}{\partial x^2} + \frac{\nu}{R^2}\frac{\partial^2 w}{\partial \theta^2}\right] \\
N_\theta &= \frac{Eh}{(1-\nu^2)}\left[\frac{1}{R}\frac{\partial v}{\partial \theta} + \frac{w}{R} + \nu\frac{\partial u}{\partial x}\right] \quad , \quad M_\theta = -\frac{Eh^3}{12(1-\nu^2)}\left[\frac{1}{R^2}\frac{\partial^2 w}{\partial \theta^2} + \nu\frac{\partial^2 w}{\partial x^2}\right] \\
N_{x\theta} = N_{\theta x} &= \frac{Eh}{2(1+\nu)}\left[\frac{\partial v}{\partial x} + \frac{1}{R}\frac{\partial u}{\partial \theta}\right] \quad , \quad M_{x\theta} = M_{\theta x} = -\frac{Eh^3}{12R(1+\nu)}\frac{\partial^2 w}{\partial x \partial \theta} \, .
\end{aligned}
\tag{2.5}
$$

Similar expressions are obtained in the higher order theories.

Strong Form of the Donnell-Mushtari Shell Equations

The equations of the dynamic equilibrium of the element are obtained by balancing the internal force and moment resultants as shown in Figure 2 with any externally applied forces and moments. Let

$$\vec{q} = \hat{q}_x \hat{\imath}_x + \hat{q}_\theta \hat{\imath}_\theta + \hat{q}_n \hat{\imath}_n$$

and

$$\vec{m} = \hat{m}_x \hat{\imath}_x + \hat{m}_\theta \hat{\imath}_\theta$$

denote the surface forces and moments due to an external field which is acting on the middle surface. Hence $\vec{q}$ and $\vec{m}$ have units of force and moment per unit area, respectively.

Considering equilibrium of the forces in the x, θ and z directions yields

$$
\begin{aligned}
R\frac{\partial N_x}{\partial x} + \frac{\partial N_{\theta x}}{\partial \theta} + R\hat{q}_x &= 0 \, , \\
\frac{\partial N_\theta}{\partial \theta} + R\frac{N_{x\theta}}{\partial x} + Q_\theta + R\hat{q}_\theta &= 0 \, , \\
R\frac{\partial Q_x}{\partial x} + \frac{\partial Q_\theta}{\partial \theta} - N_\theta + R\hat{q}_n &= 0 \, ,
\end{aligned}
\tag{2.6}
$$

respectively. In the Donnell-Mushtari theory, the transverse shearing force Q_θ is considered to be negligible in the second equation of (2.6) and is subsequently neglected when determining the final equilibrium equations. Similarly, with 0 as a reference origin, the balancing of moments with respect to θ, x and z yields

$$
\begin{aligned}
R\frac{\partial M_x}{\partial x} + \frac{\partial M_{\theta x}}{\partial \theta} - RQ_x + R\hat{m}_\theta &= 0 \, , \\
\frac{\partial M_\theta}{\partial \theta} + R\frac{\partial M_{x\theta}}{\partial x} - RQ_\theta + R\hat{m}_x &= 0 \, , \\
N_{x\theta} - N_{\theta x} - \frac{M_{\theta x}}{R} &= 0 \, ,
\end{aligned}
\tag{2.7}
$$

respectively. By referring to the integral definitions of $N_{x\theta}, N_{\theta x}$ and $M_{\theta x}$, it can be seen that the third expression in (2.7) is identically satisfied due to the symmetry of the stress tensor.

Time enters the equilibrium equations through the inertial terms; hence for time-dependent problems, the force $\hat{q}_x$ is replaced by $-\rho h \frac{\partial^2 u}{\partial t^2} + \hat{q}_x$ where ρ is the density in mass per unit volume of the shell. Similar substitutions are made for $\hat{q}_\theta$ and $\hat{q}_n$. By combining (2.6) and (2.7), one arrives at the time-dependent Donnell-Mushtari equilibrium equations for a thin cylindrical shell with radius of curvature R and thickness h

$$\begin{aligned} R\rho h \frac{\partial^2 u}{\partial t^2} - R\frac{\partial N_x}{\partial x} - \frac{\partial N_{\theta x}}{\partial \theta} &= R\hat{q}_x \\ R\rho h \frac{\partial^2 v}{\partial t^2} - \frac{\partial N_\theta}{\partial \theta} - R\frac{N_{x\theta}}{\partial x} &= R\hat{q}_\theta \\ R\rho h \frac{\partial^2 w}{\partial t^2} - R\frac{\partial^2 M_x}{\partial x^2} - \frac{1}{R}\frac{\partial^2 M_\theta}{\partial \theta^2} - 2\frac{\partial^2 M_{x\theta}}{\partial x \partial \theta} + N_\theta &= R\hat{q}_n + R\frac{\partial \hat{m}_\theta}{\partial x} + \frac{\partial \hat{m}_x}{\partial \theta} \,. \end{aligned} \tag{2.8}$$

We note that the representation of the external loads as surface moments and forces is convenient when deriving the strong form of the equations of motion. However, in many applications where it is necessary to actually determine expressions for these loads or when using the weak form of the equations, it is advantageous to represent these loads in terms of line forces and moments. To accomplish this, let $\hat{M}_x, \hat{M}_\theta, \hat{N}_x$, and $\hat{N}_\theta$ denote the external resultants acting on the edge of an infinitesimal element which have the same orientation as the internal resultants depicted in Figure 2 (with units of moment and force per unit length of middle surface). Force and moment balancing can be used to write the area moments and in-plane forces in terms of these line moments and forces, thus yielding

$$\begin{aligned} \hat{q}_x &= -\frac{\partial \hat{N}_x}{\partial x} \quad , \quad \hat{q}_\theta = -\frac{1}{R}\frac{\partial \hat{N}_\theta}{\partial \theta} \\ \hat{m}_x &= -\frac{1}{R}\frac{\partial \hat{M}_\theta}{\partial \theta} \quad , \quad \hat{m}_\theta = -\frac{\partial \hat{M}_x}{\partial x} \,. \end{aligned} \tag{2.9}$$

We point out that the first expression in (2.9) can be obtained from (2.6) simply by replacing N_x by $\hat{N}_x$ and deleting $\frac{\partial N_{\theta x}}{\partial \theta}$ in the first expression of (2.6). Similar analysis leads to the other expressions in (2.9). The use of these line moments and forces in (2.8) is equivalent to including the external resultants directly when determining the equations of moment and force equilibrium for an infinitesimal shell element as done in (2.6) and (2.7).

The substitution of the internal moments and forces in (2.5) and the external resultants from (2.9) then yields

$$\begin{aligned} \frac{1}{C_L^2}\frac{\partial^2 u}{\partial t^2} - \frac{\partial^2 u}{\partial x^2} - \frac{1-\nu}{2R^2}\frac{\partial^2 u}{\partial \theta^2} - \frac{1+\nu}{2R}\frac{\partial^2 v}{\partial x \partial \theta} - \frac{\nu}{R}\frac{\partial w}{\partial x} &= -\frac{(1-\nu^2)}{Eh}\frac{\partial \hat{N}_x}{\partial x} \\ \frac{1}{C_L^2}\frac{\partial^2 v}{\partial t^2} - \frac{1-\nu}{2}\frac{\partial^2 v}{\partial x^2} - \frac{1}{R^2}\frac{\partial^2 v}{\partial \theta^2} - \frac{1+\nu}{2R}\frac{\partial^2 u}{\partial x \partial \theta} - \frac{1}{R^2}\frac{\partial w}{\partial \theta} &= -\frac{(1-\nu^2)}{Eh}\frac{1}{R}\frac{\partial \hat{N}_\theta}{\partial \theta} \\ \frac{1}{C_L^2}\frac{\partial^2 w}{\partial t^2} + \frac{\nu}{R}\frac{\partial u}{\partial x} + \frac{1}{R^2}\frac{\partial v}{\partial \theta} + \frac{1}{R^2}w + \frac{h^2}{12}\nabla^4 w &= \frac{(1-\nu^2)}{Eh}\left[\hat{q}_n - \frac{1}{R^2}\frac{\partial^2 \hat{M}_\theta}{\partial \theta^2} - \frac{\partial \hat{M}_x}{\partial x^2}\right] \end{aligned} \tag{2.10}$$

where again, u, v and w are the axial, tangential and radial displacements, respectively [14]. The constant C_L given by

$$C_L = \left[\frac{E_s}{\rho_s(1-\nu_s^2)}\right]^{\frac{1}{2}}$$

is the phase speed of axial waves in the cylinder wall. The external line forces $\hat{N}_x$ and $\hat{N}_\theta$ and moments $\hat{M}_x$ and $\hat{M}_\theta$ have units of force and moment per unit length of middle surface, respectively, and are generated in our problem by the activation of the piezoceramic patches. The load $\hat{q}_n$ is left as a surface force since this is the form that it usually takes in problems involving the excitation of a shell through normal forces (an example of a normal force in this form is the pressure exerted on the shell due to an exterior or interior acoustic field).

We again emphasize that the resultant expressions in (2.9) (and hence the system (2.10)) were derived for an infinitesimal element; hence certain modifications must be made when considering the *global* form of the resultants and equations (as is necessary when the resultants are generated by a piezoceramic patch). In certain cases (e.g., for certain types of moments and forces), the system (2.10) agrees with the strong form of the global shell equations. In general, however, this is not true, and one must exercise extreme care in determining the form of the global representations for the moments and forces.

Weak Form of the Donnell-Mushtari Cylindrical Shell Equations

In order to find the weak form of the shell equations, the kinetic and strain energies of the shell are needed. By combining the Kirchhoff shell hypothesis with the strain results from classical elasticity theory, it follows that the strain energy stored in the shell during deformation is given by

$$U = \frac{1}{2}\int_{-h/2}^{h/2}\int_0^{2\pi}\int_0^{\ell}\left(\sigma_x e_x + \sigma_\theta e_\theta + \sigma_{x\theta}\gamma_{x\theta}\right)(1+z/R)\,R dx d\theta dz$$

where the stains and stresses are given in (2.1) and (2.4), respectively. Substitution and integration (with $(1+z/R)^{-1}$ replaced by its geometric series expansion and neglecting powers of z in the integrand which are greater than two) yields

$$\begin{aligned} U = \frac{1}{2}\int_0^{2\pi}\int_0^{\ell}\frac{Eh}{(1-\nu^2)}\Bigg\{ & \left[(\varepsilon_x+\varepsilon_\theta)^2 - 2(1-\nu)\left(\varepsilon_x\varepsilon_\theta - \frac{\varepsilon_{x\theta}^2}{4}\right)\right] \\ & + \frac{h^2}{12}\left[(\kappa_x+\kappa_\theta)^2 - 2(1-\nu)\left(\kappa_x\kappa_\theta - \frac{\tau^2}{4}\right) + \frac{2}{R}(\varepsilon_x\kappa_x - \varepsilon_\theta\kappa_\theta)\right. \\ & \left. - \frac{(1-\nu)}{2}\frac{\varepsilon_{x\theta}}{R}\tau + \frac{\varepsilon_\theta^2}{R^2} + \frac{(1-\nu)}{2}\frac{\varepsilon_{x\theta}^2}{R^2}\right]\Bigg\} R dx d\theta \,. \end{aligned}$$

With the change of variables $s = x/R$, the total strain energy can be written as

$$U = \frac{1}{2}\int_0^{2\pi}\int_0^{\ell/R}\frac{Eh}{(1-\nu^2)}\left[I_{DM} + kI_{BFL}\right] ds d\theta$$

where $k = h^2/(12R^2)$, I_{DM} is the integrand corresponding to the Donnell-Mushtari theory and I_{BFL} denotes the terms which are retained to yield the Byrne, Flügge and Lur'ye strain energy. These two components are given by

$$\begin{aligned} I_{DM} &= \left(\frac{\partial u}{\partial s} + \frac{\partial v}{\partial \theta} + w\right)^2 - 2(1-\nu)\left[\frac{\partial u}{\partial s}\left(\frac{\partial v}{\partial \theta} + w\right) - \frac{1}{4}\left(\frac{\partial v}{\partial s} + \frac{\partial u}{\partial \theta}\right)^2\right] \\ &+ k\left\{\left(\nabla^2 w\right)^2 - 2(1-\nu)\left[\frac{\partial^2 w}{\partial s^2}\frac{\partial^2 w}{\partial \theta^2} - \left(\frac{\partial^2 w}{\partial s \partial \theta}\right)^2\right]\right\} \end{aligned}$$

and

$$\begin{aligned} I_{BFL} &= -2\nu\frac{\partial v}{\partial \theta}\frac{\partial^2 w}{\partial s^2} - 3(1-\nu)\frac{\partial v}{\partial s}\frac{\partial^2 w}{\partial s \partial \theta} + \frac{3}{2}(1-\nu)\left(\frac{\partial v}{\partial s}\right)^2 + (1-\nu)\frac{\partial u}{\partial \theta}\frac{\partial^2 w}{\partial s \partial \theta} \\ &+ \frac{1}{2}(1-\nu)\left(\frac{\partial u}{\partial \theta}\right)^2 - 2\frac{\partial u}{\partial s}\frac{\partial^2 w}{\partial s^2} + 2w\frac{\partial^2 w}{\partial \theta^2} + w^2 \, . \end{aligned}$$

For simplicity of presentation, a weak form of the shell equations will be developed using the Donnell-Mushtari strain expression; a corresponding set of equations can be derived in a similar manner in the Byrne, Flügge and Lur'ye case.

The kinetic energy of the shell is given by

$$T = \frac{1}{2}\int_0^{2\pi}\int_0^{\ell/R} \rho h\left[\left(\frac{\partial^2 u}{\partial t^2}\right)^2 + \left(\frac{\partial^2 v}{\partial t^2}\right)^2 + \left(\frac{\partial^2 w}{\partial t^2}\right)^2\right] R^2 ds d\theta \, .$$

Throughout this development, it is assumed that the shell satisfies *shear diaphragm* boundary conditions at $x = 0, \ell$; that is, it is assumed that

$$v = w = N_x = M_x = 0$$

at the ends. This is done merely to demonstrate the equivalence between the weak form which follows and the strong form already discussed; other boundary conditions can be treated with similar arguments. It should be noted that the conditions $v = w = 0$ at the ends are essential boundary conditions and hence must be enforced on the chosen state space.

For an arbitrary time interval $[t_0, t_1]$, consider the action integral

$$A[\vec{u}] = \int_{t_0}^{t_1} (T - U)dt \tag{2.11}$$

where $\vec{u} = [u, v, w]$ is considered in the space $V = H_b^1(\Omega) \times H_b^1(\Omega) \times H_b^2(\Omega)$. Here Ω denotes the shell and the subscript b denotes the set of functions satisfying the essential boundary conditions. One then considers variations of the form

$$\hat{u} = \vec{u} + \varepsilon\vec{\Phi} = \begin{bmatrix} u(t,r,\theta,x) \\ v(t,r,\theta,x) \\ w(t,r,\theta,x) \end{bmatrix} + \varepsilon \begin{bmatrix} \eta_1(t)\phi_1(r,\theta,x) \\ \eta_2(t)\phi_2(r,\theta,x) \\ \eta_3(t)\phi_3(r,\theta,x) \end{bmatrix} .$$

Here $\vec{\eta} = [\eta_1, \eta_2, \eta_3]$ and $\vec{\phi} = [\phi_1, \phi_2, \phi_3]$ are chosen so that

i.) $\hat{u}(t,\cdot,\cdot,\cdot) \in V$

ii.) $\hat{u}(t_0,\cdot,\cdot,\cdot) = \hat{u}(t_1,\cdot,\cdot,\cdot)$.

Note that this enforces $\vec{\eta} \in [H^2(0,T)]^3$, $\vec{\eta}(t_0) = \vec{\eta}(t_1)$ and $\vec{\phi} \in V$.

Hamilton's principle states that the motion of the shell must give a stationary value to the action integral when compared to variations in the motion, thus leading to the requirement that for all $\vec{\Phi}$,

$$\frac{d}{d\varepsilon} A\left[\vec{u} + \varepsilon\vec{\Phi}\right]\Big|_{\varepsilon=0} = 0 \quad .$$

With the definition (2.11) for the action integral, Hamilton's principle leads to the condition

$$\begin{aligned}
0 = \frac{\partial}{\partial\varepsilon} A[\hat{u}]\Big|_{\varepsilon=0} \;=\; & \int_{t_0}^{t_1}\int_0^{2\pi}\int_0^{\ell/R} \rho h\left[\frac{\partial u}{\partial t}\frac{\partial \eta_1}{\partial t}\phi_1 + \frac{\partial v}{\partial t}\frac{\partial \eta_2}{\partial t}\phi_2 + \frac{\partial w}{\partial t}\frac{\partial \eta_3}{\partial t}\phi_3\right] R^2 ds d\theta dt \\
& - \int_{t_0}^{t_1}\int_0^{2\pi}\int_0^{\ell/R} \frac{Eh}{(1-\nu^2)}\Bigg\{\left(\frac{\partial u}{\partial s} + \frac{\partial v}{\partial \theta} + w\right)\left(\eta_1\frac{\partial \phi_1}{\partial s} + \eta_2\frac{\partial \phi_2}{\partial \theta} + \eta_3\phi_3\right) \\
& \qquad -(1-\nu)\Bigg[\eta_1 w\frac{\partial \phi_1}{\partial s} + \eta_1\frac{\partial v}{\partial \theta}\frac{\partial \phi_1}{\partial s} + \eta_2\frac{\partial u}{\partial s}\frac{\partial \phi_2}{\partial \theta} + \eta_3\frac{\partial u}{\partial s}\phi_3 \\
& \qquad\qquad -\frac{1}{2}\left(\frac{\partial v}{\partial s} + \frac{\partial u}{\partial \theta}\right)\left(\eta_2\frac{\partial \phi_2}{\partial s} + \eta_1\frac{\partial \phi_1}{\partial \theta}\right)\Bigg] \\
& \qquad + k\Bigg\{\eta_3\nabla^2 w\nabla^2\phi_3 - (1-\nu)\Bigg[\eta_3\frac{\partial^2 w}{\partial\theta^2}\frac{\partial^2\phi_3}{\partial s^2} + \eta_3\frac{\partial^2 w}{\partial s^2}\frac{\partial^2\phi_3}{\partial\theta^2} \\
& \qquad\qquad -2\eta_3\frac{\partial^2 w}{\partial s\partial\theta}\frac{\partial^2\phi_3}{\partial s\partial\theta}\Bigg]\Bigg\}\Bigg\} ds d\theta dt \quad .
\end{aligned}$$

Note that this must hold for all arbitrary intervals $[t_0, t_1]$ and all admissible perturbations. Temporal integration by parts in the first integral in conjunction with the underlying condition

that $\vec{\eta}(t_0) = \vec{\eta}(t_1)$ then yields the coupled system of equations

$$\int_{t_0}^{t_1} \eta_1(t) \int_0^{2\pi} \int_0^{\ell/R} \left\{ -\frac{\rho(1-\nu^2)}{E} \frac{\partial^2 u}{\partial t^2} \phi_1 R^2 - \left(\frac{\partial u}{\partial s} + \frac{\partial v}{\partial \theta} + w \right) \frac{\partial \phi_1}{\partial s} \right.$$
$$\left. + (1-\nu) \left[w \frac{\partial \phi_1}{\partial s} + \frac{\partial v}{\partial \theta} \frac{\partial \phi_1}{\partial s} - \frac{1}{2} \left(\frac{\partial v}{\partial s} + \frac{\partial u}{\partial \theta} \right) \frac{\partial \phi_1}{\partial \theta} \right] \right\} ds d\theta dt = 0$$

$$\int_{t_0}^{t_1} \eta_2(t) \int_0^{2\pi} \int_0^{\ell/R} \left\{ -\frac{\rho(1-\nu^2)}{E} \frac{\partial^2 v}{\partial t^2} \phi_2 R^2 - \left(\frac{\partial u}{\partial s} + \frac{\partial v}{\partial \theta} + w \right) \frac{\partial \phi_2}{\partial \theta} \right.$$
$$\left. + (1-\nu) \left[\frac{\partial u}{\partial s} \frac{\partial \phi_2}{\partial \theta} - \frac{1}{2} \left(\frac{\partial v}{\partial s} + \frac{\partial u}{\partial \theta} \right) \frac{\partial \phi_2}{\partial s} \right] \right\} ds d\theta dt = 0$$

$$\int_{t_0}^{t_1} \eta_3(t) \int_0^{2\pi} \int_0^{\ell/R} \left\{ -\frac{\rho(1-\nu^2)}{E} \frac{\partial^2 w}{\partial t^2} \phi_3 R^2 - \left(\frac{\partial u}{\partial s} + \frac{\partial v}{\partial \theta} + w \right) \phi_3 + (1-\nu) \frac{\partial u}{\partial s} \phi_3 \right.$$
$$\left. - k \left\{ \nabla^2 w \nabla^2 \phi_3 - (1-\nu) \left[\frac{\partial^2 w}{\partial \theta^2} \frac{\partial^2 \phi_3}{\partial s^2} + \frac{\partial^2 w}{\partial s^2} \frac{\partial^2 \phi_3}{\partial \theta^2} - 2 \frac{\partial^2 w}{\partial s \partial \theta} \frac{\partial^2 \phi_3}{\partial s \partial \theta} \right] \right\} \right\} ds d\theta dt = 0 \, .$$

The weak form of the equations of motion for the unforced shell is thus

$$\int_0^{2\pi} \int_0^{\ell/R} \left\{ \frac{R^2}{C_L^2} \frac{\partial^2 u}{\partial t^2} \phi_1 + \left(\frac{\partial u}{\partial s} + \nu \frac{\partial v}{\partial \theta} + \nu w \right) \frac{\partial \phi_1}{\partial s} + \frac{1}{2}(1-\nu) \left(\frac{\partial v}{\partial s} + \frac{\partial u}{\partial \theta} \right) \frac{\partial \phi_1}{\partial \theta} \right\} ds d\theta = 0$$

$$\int_0^{2\pi} \int_0^{\ell/R} \left\{ \frac{R^2}{C_L^2} \frac{\partial^2 v}{\partial t^2} \phi_2 + \left(\nu \frac{\partial u}{\partial s} + \frac{\partial v}{\partial \theta} + w \right) \frac{\partial \phi_2}{\partial \theta} + \frac{1}{2}(1-\nu) \left(\frac{\partial v}{\partial s} + \frac{\partial u}{\partial \theta} \right) \frac{\partial \phi_2}{\partial s} \right\} ds d\theta = 0$$

$$\int_0^{2\pi} \int_0^{\ell/R} \left\{ \frac{R^2}{C_L^2} \frac{\partial^2 w}{\partial t^2} \phi_3 + \left(\nu \frac{\partial u}{\partial s} + \frac{\partial v}{\partial \theta} + w \right) \phi_3 \right.$$
$$\left. + k \left\{ \nabla^2 w \nabla^2 \phi_3 - (1-\nu) \left[\frac{\partial^2 w}{\partial \theta^2} \frac{\partial^2 \phi_3}{\partial s^2} + \frac{\partial^2 w}{\partial s^2} \frac{\partial^2 \phi_3}{\partial \theta^2} - 2 \frac{\partial^2 w}{\partial s \partial \theta} \frac{\partial^2 \phi_3}{\partial s \partial \theta} \right] \right\} \right\} ds d\theta = 0$$

for all $\vec{\phi} \in V$. Again, the constant $C_L = \left[\frac{E}{\rho(1-\nu^2)} \right]^{1/2}$ is the phase speed of axial waves in the cylinder wall.

In terms of the moment and force resultants (see (2.5)) and the original axial variable x, the weak form is

$$\int_0^{2\pi} \int_0^{\ell} \left\{ R\rho h \frac{\partial^2 u}{\partial t^2} \phi_1 + R N_x \frac{\partial \phi_1}{\partial x} + N_{\theta x} \frac{\partial \phi_1}{\partial \theta} \right\} dx d\theta = 0$$

$$\int_0^{2\pi} \int_0^{\ell} \left\{ R\rho h \frac{\partial^2 v}{\partial t^2} \phi_2 + N_\theta \frac{\partial \phi_2}{\partial \theta} + R N_{x\theta} \frac{\partial \phi_2}{\partial x} \right\} dx d\theta = 0 \qquad (2.12)$$

$$\int_0^{2\pi} \int_0^{\ell} \left\{ R\rho h \frac{\partial^2 w}{\partial t^2} \phi_3 + N_\theta \phi_3 - R M_x \frac{\partial^2 \phi_3}{\partial x^2} - \frac{1}{R} M_\theta \frac{\partial^2 \phi_3}{\partial \theta^2} - 2 M_{x\theta} \frac{\partial^2 \phi_3}{\partial x \partial \theta} \right\} dx d\theta = 0 \, .$$

The derivation thus far has been for the unforced shell. To include the contributions of applied external forces and moments which do nonconservative work on the shell, one can appeal to an extended form of Hamilton's principle or more formally include these contributions directly in the system (2.12). Both techniques yield identical final equations and for ease of presentation, we will take the latter approach.

The inclusion of the applied line forces and moments $\hat{N}_x, \hat{N}_\theta$ and $\hat{M}_x, \hat{M}_\theta$ and the surface load $\hat{q}_n$ in the system then yields

$$\begin{aligned}
&\int_0^{2\pi}\int_0^{\ell}\left\{R\rho h\frac{\partial^2 u}{\partial t^2}\phi_1 + RN_x\frac{\partial\phi_1}{\partial x} + N_{\theta x}\frac{\partial\phi_1}{\partial\theta} - R\hat{N}_x\frac{\partial\phi_1}{\partial x}\right\}dxd\theta = 0\\
&\int_0^{2\pi}\int_0^{\ell}\left\{R\rho h\frac{\partial^2 v}{\partial t^2}\phi_2 + N_\theta\frac{\partial\phi_2}{\partial\theta} + RN_{x\theta}\frac{\partial\phi_2}{\partial x} - \hat{N}_\theta\frac{\partial\phi_2}{\partial\theta}\right\}dxd\theta = 0\\
&\int_0^{2\pi}\int_0^{\ell}\left\{R\rho h\frac{\partial^2 w}{\partial t^2}\phi_3 + N_\theta\phi_3 - RM_x\frac{\partial^2\phi_3}{\partial x^2} - \frac{1}{R}M_\theta\frac{\partial^2\phi_3}{\partial\theta^2} - 2M_{x\theta}\frac{\partial^2\phi_3}{\partial x\partial\theta}\right.\\
&\qquad\left. -R\hat{q}_n\phi_3 + R\hat{M}_x\frac{\partial^2\phi_3}{\partial x^2} + \frac{1}{R}\hat{M}_\theta\frac{\partial^2\phi_3}{\partial\theta^2}\right\}dxd\theta = 0
\end{aligned} \tag{2.13}$$

for all $\vec{\phi} \in V$ as the weak form of the Donnell-Mushtari equations of motion for the forced shell.

With the assumption of sufficient smoothness, the weak solution in this form is consistent with the strong solution in (2.8). The vanishing of several of the boundary terms which arise during integration by parts is a result of the choice $V = H_b^1(\Omega) \times H_b^1(\Omega) \times H_b^2(\Omega)$ for the function space since the state variables and test functions are required to satisfy the essential boundary conditions

$$v = w = 0$$

at $x = 0, \ell$.

We point out that in the weak form (2.13), one is not required to differentiate the applied force and moment resultants $\hat{N}_x, \hat{N}_\theta, \hat{M}_x$ and $\hat{M}_\theta$ as is required in the strong form (2.10). This proves to be very beneficial when these terms are generated by finite piezoceramic patches as discussed in the next section.

Plate Equations

Consider a thin rectangular plate whose edges lie along the coordinate lines $x = 0, \ell$ and $y = 0, a$. We assume that the plate subjected to both longitudinal and transverse loading via the surface forces and moments $\hat{q}_x, \hat{q}_\theta, \hat{q}_n$ and $\hat{m}_x, \hat{m}_\theta$. With u, v and w denoting the displacements in the x, y and normal directions, respectively, the strong form of the Kirchhoff plate equations is given by

$$\rho h\frac{\partial^2 u}{\partial t^2} - \frac{\partial N_x}{\partial x} - \frac{\partial N_{yx}}{\partial y} = \hat{q}_x$$

$$\rho h\frac{\partial^2 v}{\partial t^2} - \frac{\partial N_y}{\partial y} - \frac{N_{xy}}{\partial x} = \hat{q}_y \tag{2.14}$$

$$\rho h\frac{\partial^2 w}{\partial t^2} - \frac{\partial^2 M_x}{\partial x^2} - \frac{\partial^2 M_y}{\partial y^2} - \frac{\partial^2 M_{xy}}{\partial x \partial y} - \frac{\partial^2 M_{yx}}{\partial y \partial x} = \hat{q}_n + \frac{\partial \hat{m}_x}{\partial y} + \frac{\partial \hat{m}_y}{\partial x}$$

where the moment and force resultants are

$$N_x = \frac{Eh}{1-\nu^2}\left(\frac{\partial u}{\partial x} + \nu\frac{\partial v}{\partial y}\right) \quad , \quad M_x = -\frac{Eh^3}{12(1-\nu^2)}\left(\frac{\partial^2 w}{\partial x^2} + \nu\frac{\partial^2 w}{\partial y^2}\right)$$

$$N_y = \frac{Eh}{1-\nu^2}\left(\frac{\partial v}{\partial y} + \nu\frac{\partial u}{\partial x}\right) \quad , \quad M_y = -\frac{Eh^3}{12(1-\nu^2)}\left(\frac{\partial^2 w}{\partial y^2} + \nu\frac{\partial^2 w}{\partial x^2}\right)$$

$$N_{xy} = N_{yx} = \frac{Eh}{2(1+\nu)}\left(\frac{\partial v}{\partial x} + \frac{\partial u}{\partial y}\right) \quad , \quad M_{xy} = M_{yx} = -\frac{Eh^3}{12(1+\nu)}\frac{\partial^2 w}{\partial x \partial y} .$$

The first two equations in (2.14) describe the longitudinal movement of the plate while the third equation describes the transverse motion of the plate.

To find the weak form of the equations, the vector $\vec{u} = [u, v, w]$ containing the displacements in the x, y and normal directions is considered in the space $V = H_b^1(\Omega) \times H_b^1(\Omega) \times H_b^2(\Omega)$ where Ω denotes the plate and the subscript b denotes the set of functions satisfying essential boundary conditions for a specific problem. By using analysis similar to that just described for cylindrical shells, the weak form of the equations of motion for the plate can be found to be

$$\int_0^a \int_0^\ell \left\{\rho h\frac{\partial^2 u}{\partial t^2}\phi_1 + N_x\frac{\partial \phi_1}{\partial x} + N_{yx}\frac{\partial \phi_1}{\partial y} - \hat{N}_x\frac{\partial \phi_1}{\partial x}\right\} dxdy = 0$$

$$\int_0^a \int_0^\ell \left\{\rho h\frac{\partial^2 v}{\partial t^2}\phi_2 + N_y\frac{\partial \phi_2}{\partial y} + N_{xy}\frac{\partial \phi_2}{\partial x} - \hat{N}_y\frac{\partial \phi_2}{\partial y}\right\} dxdy = 0$$

$$\int_0^a \int_0^\ell \left\{\rho h\frac{\partial^2 w}{\partial t^2}\phi_3 - M_x\frac{\partial^2 \phi_3}{\partial x^2} - M_y\frac{\partial^2 \phi_3}{\partial y^2} - M_{xy}\frac{\partial^2 \phi_3}{\partial x \partial y} - M_{yx}\frac{\partial^2 \phi_3}{\partial x \partial y}\right.$$
$$\left. -\hat{q}_n\phi_3 + \hat{M}_x\frac{\partial^2 \phi_3}{\partial x^2} + \hat{M}_y\frac{\partial^2 \phi_3}{\partial y^2}\right\} dxdy = 0 \tag{2.15}$$

for all $\vec{\phi} = [\phi_1, \phi_2, \phi_3] \in V$. As in the case of the thin shell, the external line forces and moments $\hat{N}_x, \hat{N}_y, \hat{M}_x$ and $\hat{M}_y$ are related in an infinitesimal sense to the corresponding area forces and moments $\hat{q}_x, \hat{q}_y, \hat{m}_y$ and $\hat{m}_x$ appearing in the strong form of the equations by the relations

$$\hat{q}_x = -\frac{\partial \hat{N}_x}{\partial x} \quad , \quad \hat{q}_y = -\frac{\partial \hat{N}_y}{\partial y}$$
$$\hat{m}_x = -\frac{\partial \hat{M}_y}{\partial y} \quad , \quad \hat{m}_y = -\frac{\partial \hat{M}_x}{\partial x} . \tag{2.16}$$

If the solution has sufficient smoothness, integration by parts can be used to show that the weak solution is consistent with the strong solution in (2.14).

Beam Equations

The motion of an undamped thin beam of length ℓ and width 1 can be determined from the dynamics of thin plate theory by considering only the vibrations in the x-direction along with the usual transverse vibrations (in the z direction). From (2.14) this yields the strong form of the Euler-Bernoulli beam equations

$$\begin{aligned} \rho h \frac{\partial^2 u}{\partial t^2} - \frac{\partial N_x}{\partial x} &= \hat{q}_x \ , \\ \rho h \frac{\partial^2 w}{\partial t^2} - \frac{\partial^2 M_x}{\partial x^2} &= \hat{q}_n + \frac{\partial \hat{m}_y}{\partial x} \end{aligned} \tag{2.17}$$

where

$$N_x = Eh \frac{\partial u}{\partial x}$$

$$M_x = -\frac{Eh^3}{12} \frac{\partial^2 w}{\partial x^2} = -EI \frac{\partial^2 w}{\partial x^2} \ .$$

Note that $I = h^3/12$ is the moment of inertia for a beam of width 1.

A corresponding weak or variational form of the equations can be determined by choosing $V = H_b^1(\Omega) \times H_b^2(\Omega)$ for the space of trial functions where Ω denotes the beam and the subscript b again denotes the set of functions which must satisfy the essential boundary conditions. Through either an energy derivation such as that given for the thin shell, or simply integration by parts, one arrives at the variational form

$$\begin{aligned} &\int_0^\ell \left\{ \rho h \frac{\partial^2 u}{\partial t^2} \phi_1 + N_x \frac{\partial \phi_1}{\partial x} - \hat{N}_x \frac{\partial \phi_1}{\partial x} \right\} dx = 0 \quad \text{for all} \ \ \phi_1 \in H_b^1(\Omega) \\ &\int_0^\ell \left\{ \rho h \frac{\partial^2 w}{\partial t^2} \phi_3 - M_x \frac{\partial^2 \phi_3}{\partial x^2} - \hat{q}_n \phi_3 + \hat{M}_x \frac{\partial^2 \phi_3}{\partial x^2} \right\} dx = 0 \quad \text{for all} \ \ \phi_3 \in H_b^2(\Omega) \end{aligned} \tag{2.18}$$

of the beam equations. We point out that in this form, one is not required to differentiate the external force or moment resultants, $\hat{N}_x$ and $\hat{M}_x$, which proves to be very useful when these terms are generated by the activation of finite piezoceramic patches.

3 Patch Contributions to the Shell Equations

For a thin cylindrical shell, the strong and weak forms of the equations of motion are given by (2.8) and (2.13), respectively. In the case of the weak form, it is seen that the loads can be written in terms of the line forces and moments $\hat{N}_x, \hat{N}_\theta, \hat{M}_x$ and $\hat{M}_\theta$ and the normal surface load $\hat{q}_n$, while the strong form contains surface loads and the derivatives of surface

moments. In the problem under consideration, these quantities result from the activation of piezoceramic patches of thickness T which are assumed to be perfectly bonded to a cylindrical shell of thickness h with midsurface radius R (see Figure 3). As shown in Figure 4, the patches are assumed to be situated so that their edges are parallel to lines of constant x and θ. Because the patches generate no shear strains, the exterior load $\hat{q}_n$ is taken to be $\hat{q}_n = 0$. If the weak form (2.13) is used, the external line moments and forces are simply

$$\begin{aligned} \hat{M}_x &= (M_x)_{pe} \quad , \quad \hat{M}_\theta = (M_\theta)_{pe} \\ \hat{N}_x &= (N_x)_{pe} \quad , \quad \hat{N}_\theta = (N_\theta)_{pe} \end{aligned} \tag{3.1}$$

where $(M_x)_{pe}, (M_\theta)_{pe}, (N_x)_{pe}$ and $(N_\theta)_{pe}$ are the respective moments and in-plane forces which are generated by the patches. The subscript pe is used to denote patch properties and to help differentiate them from shell properties which have no subscript. When it is necessary to differentiate between the two patches, the outer will be denoted with a subscript pe_1 with a subscript pe_2 being used to denote the inner patch.

However, if one is using the strong form (2.8) of the equations of motion with piezoceramic actuators, the surface moments and forces to be used in (2.8) are given by

$$\begin{aligned} \hat{m}_x &= -\frac{1}{R}\frac{\partial (M_\theta)_{pe}}{\partial \theta} \quad , \quad \hat{m}_\theta = -\frac{\partial (M_x)_{pe}}{\partial x} \\ \hat{q}_x &= -S_{1,2}(x)\hat{S}_{1,2}(\theta)\frac{\partial (N_x)_{pe}}{\partial x} \quad , \quad \hat{q}_\theta = -S_{1,2}(x)\hat{S}_{1,2}(\theta)\frac{1}{R}\frac{\partial (N_\theta)_{pe}}{\partial \theta} \ . \end{aligned} \tag{3.2}$$

For a patch with uniform thickness and bounding values x_1, x_2, θ_1 and θ_2, the presence of the indicator function

$$S_{1,2}(x) = \begin{cases} 1 & , \quad x < (x_1 + x_2)/2 \\ 0 & , \quad x = (x_1 + x_2)/2 \\ -1 & , \quad x > (x_1 + x_2)/2 \end{cases} \tag{3.3}$$

derives from the fact that the forces generated by the patch in the x-direction are antisymmetric (equal in magnitude but opposite in sign) about the line $\bar{x} = (x_1 + x_2)/2$. The same holds true for the forces in the θ-direction with $\hat{S}_{1,2}(\theta)$ being defined in an analogous manner to $S_{1,2}(x)$ in (3.3).

We point out that the differences between the external surface force expressions in (2.9) and (3.2) are due to the fact that the former were derived for an infinitesimal element whereas the latter are global expressions which preserve the overall signs of the forces generated by the patches as well as reflect the discontinuities due to changes in sign. These differences result from the property that the sense of the forces is highly dependent on the specified location of the axis origin on the neutral surface. Hence the direction of forces throughout the patch differs in some locations from those observed in the infinitesimal element thus necessitating the inclusion of the indicator functions in (3.2).

Unlike the forces, the action of the moments is specified with respect to a fixed point on the neutral surface (the point 0 for the element in Figure 2 or a point on the left edge of the shell in Figure 1). As long as the orientation of the infinitesimal element and full shell with patches are the same, the line moments derived for the infinitesimal element will be consistent with those of the full structure. Thus the expressions for the general infinitesimal moments in (2.9) need no modifications when describing the surface moments generated by the patches as given in (3.2).

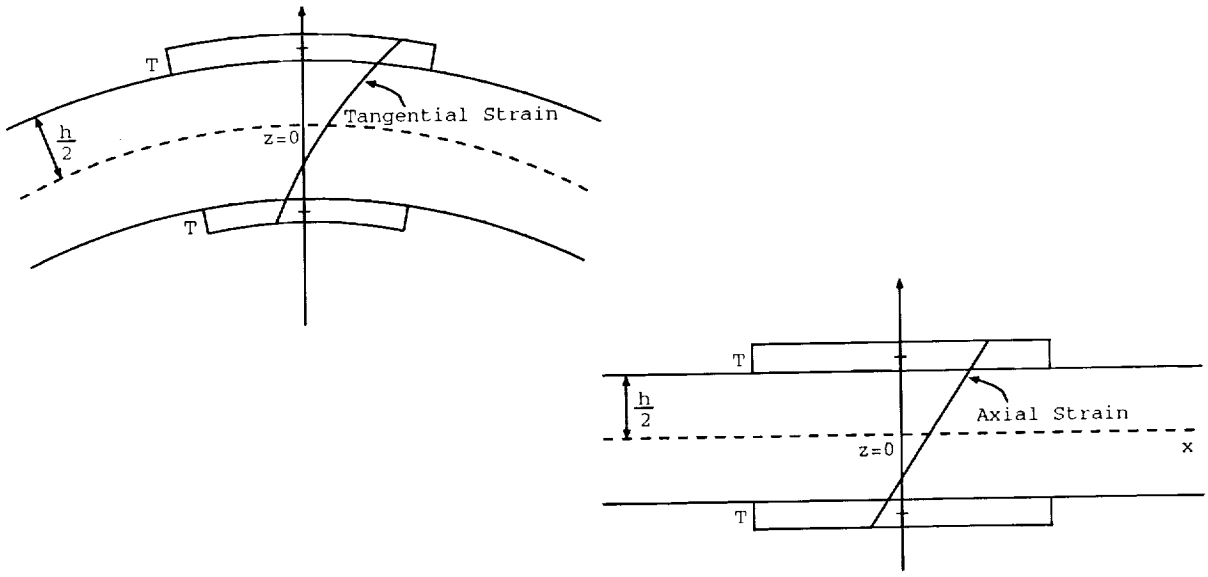

Figure 3. Strain Distribution for the Composite Structure.

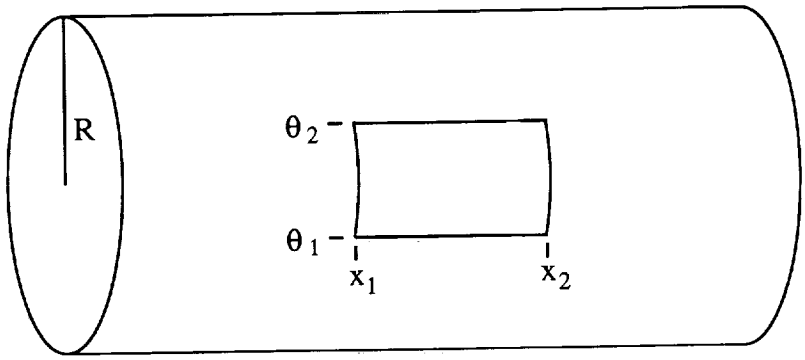

Figure 4. Piezoceramic Patch Placement.

In order to determine $(M_x)_{pe}, (M_\theta)_{pe}, (N_x)_{pe}$ and $(N_\theta)_{pe}$ and hence the loads on the shell, it is useful to write them in terms of the normal strains $\varepsilon_x, \varepsilon_\theta$ and midsurface changes in curvature κ_x, κ_θ of the middle surface ($z = 0$) of the cylindrical shell. That is, we want to express the patch moments and forces in terms of the reference surface characteristics of the cylindrical shell.

We emphasize that due to the presence and activating nature of the patches when a voltage is applied, the normal strains and changes in curvature are no longer given by the expressions in (2.3) which were derived for a homogeneous thin cylindrical shell. At this point, $\varepsilon_x, \varepsilon_\theta, \kappa_x$ and κ_θ are considered to be unknown and are determined by formulating stress-strain relations in the patch and shell followed by the balancing of moments and forces in the combined structure. In this manner, expressions for these midsurface characteristics (and hence the resulting patch moments and forces) can be found in terms of the material properties of the shell and patch, the radius of curvature of the shell, and the voltages being applied to the patches.

Stress-Strain Relations in the Patch

From (2.1), the infinitesimally exact strain relationships for a cylindrical shell with midsurface radius R are given by

$$\begin{aligned} e_x &= (\varepsilon_x + z\kappa_x) \\ e_\theta &= \frac{1}{1 + z/R}(\varepsilon_\theta + z\kappa_\theta) \end{aligned} \tag{3.4}$$

where e_x and e_θ are the normal strains at an arbitrary point on the cylindrical shell. If the patches and cylindrical shell are thin in comparison with the radius of curvature of the shell, then it is reasonable to assume that the relationship (3.4) is maintained throughout the combined thickness $h + 2T$ as shown in Figure 3 (see also [12]). Hence we will take

$$\begin{aligned} (e_x)_{pe} &= (\varepsilon_x + z\kappa_x) \\ (e_\theta)_{pe} &= \frac{1}{1 + z/R}(\varepsilon_\theta + z\kappa_\theta) \end{aligned} \tag{3.5}$$

where $(e_x)_{pe}$ and $(e_\theta)_{pe}$ are the normal strains at an arbitrary point on the patch. Note that this assumption implies that the strains at the interface are continuous and that the centers for the radii of curvature for the shell and patch are concurrent. As seen in (3.4) and (3.5), the tangential strain distribution in the shell and patch is in general nonlinear in z (see also Figure 3).

We point out that the model at this point differs from the flat plate piezoceramic coupling model [15] both in the presence of the term z/R in the tangential strain expression of (3.5) and in the fact that the model retains the coupling between the normal midsurface strains and the changes in curvature (this is analogous to simultaneously considering both longitudinal and transverse vibrations in a plate). Although the ratio z/R is neglected when deriving the Donnell-Mushtari model (see (2.2)), we retain it here so that curvature effects are fully included in the coupling between the patch and shell. The retention of this term also ensures that the patch interaction model can be directly applied to higher order shell models without necessitating changes to accommodate the greater accuracy.

From the constitutive relations in (2.4), it can be seen that the stress distributions within the cylindrical shell are

$$\begin{aligned} \sigma_x &= \frac{E}{1 - \nu^2}(e_x + \nu e_\theta) \\ \sigma_\theta &= \frac{E}{1 - \nu^2}(e_\theta + \nu e_x) \ . \end{aligned} \tag{3.6}$$

The stress distribution in the patches will contain contributions from both the free piezoceramic actuator strain and the strain distribution in (3.5). At this point we assume that when voltage is applied and the patch is activated, in accordance with basic shell theory, equal strains are induced in the x and θ directions and the radius of curvature is not changed in either direction. Patches satisfying this assumption could be made, for example, by taking a portion of a thin-walled tubular piezoceramic element. For the outer patch, the magnitude of the induced free strains is then taken to be

$$e_{pe_1} = (e_x)_{pe_1} = (e_\theta)_{pe_1} = \frac{d_{31}}{T} V_1$$

where d_{31} is a piezoceramic strain constant and V_1 is the applied voltage. We point out that when a voltage is applied to a patch with edge coordinates x_1, x_2, θ_1 and θ_2, the point $(\bar{x}, \bar{\theta}) = ((x_1 + x_2)/2, R(\theta_1 + \theta_2)/2)$ will not move whereas the axially symmetric points on either side will move an equal amount in opposite directions. This motivates the use of the indicator functions at various points throughout the development

Assuming that the two patches have the same Young's modulus, E_{pe}, and Poisson's ratio, ν_{pe}, the stress distribution in the outer patch is given by

$$\begin{aligned}(\sigma_x)_{pe_1} &= \frac{E_{pe}}{1-\nu_{pe}^2}\left(e_x + \nu_{pe} e_\theta - (1+\nu_{pe}) e_{pe_1}\right) \\ (\sigma_\theta)_{pe_1} &= \frac{E_{pe}}{1-\nu_{pe}^2}\left(e_\theta + \nu_{pe} e_x - (1+\nu_{pe}) e_{pe_1}\right)\end{aligned} \tag{3.7}$$

with the negative signs resulting from conservation of forces. Similar expressions are used for the induced free strain and stress distribution in the inner patch. By comparing (3.6) and (3.7), it can be noted that a stress discontinuity occurs at the interface due to the different material properties of the shell and patch.

Moments and Forces in the Patches

By integrating the stresses over the face of a fundamental element, it follows that the moment and force resultants for the patches can be expressed as

$$\begin{aligned}(M_x)_{pe_1} &= \int_{h/2}^{h/2+T} (\sigma_x)_{pe_1}\left(1+\frac{z}{R}\right) z dz \quad , \quad (M_x)_{pe_2} = \int_{-h/2-T}^{-h/2} (\sigma_x)_{pe_2}\left(1+\frac{z}{R}\right) z dz \\ (M_\theta)_{pe_1} &= \int_{h/2}^{h/2+T} (\sigma_\theta)_{pe_1} z dz \quad , \quad (M_\theta)_{pe_2} = \int_{-h/2-T}^{-h/2} (\sigma_\theta)_{pe_2} z dz \\ (N_x)_{pe_1} &= \int_{h/2}^{h/2+T} (\sigma_x)_{pe_1}\left(1+\frac{z}{R}\right) dz \quad , \quad (N_x)_{pe_2} = \int_{-h/2-T}^{-h/2} (\sigma_x)_{pe_2}\left(1+\frac{z}{R}\right) dz \\ (N_\theta)_{pe_1} &= \int_{h/2}^{h/2+T} (\sigma_\theta)_{pe_1} dz \quad , \quad (N_\theta)_{pe_2} = \int_{-h/2-T}^{-h/2} (\sigma_\theta)_{pe_2} dz\end{aligned} \tag{3.8}$$

with units of moment per unit length and force per unit length, respectively. The explicit dependence of the patch's moment and force resultants on the shell midsurface characteristics $\varepsilon_x, \varepsilon_\theta, \kappa_x$ and κ_θ can be seen by combining (3.5), (3.7) and (3.8) (we again point out that the midsurface strains $\varepsilon_x, \varepsilon_\theta$ and curvature changes κ_x, κ_θ are unknown and will be determined by balancing moments and forces in the combined structure).

Patch Loadings

It should be noted that throughout this development, edge effects due to the patches have been ignored and thus the expressions in (3.8) apply to patches covering the full circumference of the shell and having infinite axial length. The equations can be modified for finite patches

in the following manner. For a patch with bounding values x_1, x_2, θ_1 and θ_2 as shown in Figure 4, the total line moments and forces are

$$\begin{aligned}
(M_x)_{pe} &= [(M_\theta)_{pe_1} + (M_\theta)_{pe_2}]\,[H_1(x) - H_2(x)]\,[H_1(\theta) - H_2(\theta)] \\
(M_\theta)_{pe} &= [(M_x)_{pe_1} + (M_x)_{pe_2}]\,[H_1(x) - H_2(x)]\,[H_1(\theta) - H_2(\theta)] \\
(N_x)_{pe} &= [(N_x)_{pe_1} + (N_x)_{pe_2}]\,[H_1(x) - H_2(x)]\,[H_1(\theta) - H_2(\theta)]\,S_{1,2}(x)\hat{S}_{1,2}(\theta) \\
(N_\theta)_{pe} &= [(N_\theta)_{pe_1} + (N_\theta)_{pe_2}]\,[H_1(x) - H_2(x)]\,[H_1(\theta) - H_2(\theta)]\,S_{1,2}(x)\hat{S}_{1,2}(\theta)
\end{aligned} \tag{3.9}$$

where H is the Heaviside function and $H_i(x) \equiv H(x - x_i)$, $i = 1, 2$, with a similar definition in θ. The indicator functions $S_{1,2}(x)$ and $\hat{S}_{1,2}(\theta)$ (see (3.3)) again derive from the property that for homogeneous patches having uniform thickness, opposite but equal strains are generated about the point $(\bar{x}, \bar{\theta}) = ((x_1 + x_2)/2, R(\theta_1 + \theta_2)/2)$ in the two coordinate directions.

The combination of the expressions (3.8) and (3.9) yields the patch moments and forces $(M_x)_{pe}, (M_\theta)_{pe}, (N_x)_{pe}$ and $(N_\theta)_{pe}$ in terms of the middle surface characteristics of the the cylindrical shell. Integrating the expressions in (3.8) is somewhat cumbersome however, and the procedure can be facilitated by determining the patch moments and forces in terms of the resultants of the forced shell. To accomplish this, force and moment balancing is employed.

Determination of the Patch Moments and Forces

The application of moment equilibrium about the center of the shell yields the two conditions

$$\begin{aligned}
M_x + (M_x)_{pe_1} + (M_x)_{pe_2} &= 0 \\
M_\theta + (M_\theta)_{pe_1} + (M_\theta)_{pe_2} &= 0
\end{aligned} \tag{3.10}$$

where M_x and M_θ are shell moments. Similarly, force equilibrium in the x and θ directions yields

$$\begin{aligned}
N_x + (N_x)_{pe_1} + (N_x)_{pe_2} &= 0 \\
N_\theta + (N_\theta)_{pe_1} + (N_\theta)_{pe_2} &= 0\ .
\end{aligned} \tag{3.11}$$

Thus the total patch resultants can be expressed as

$$(M_x)_{pe_1} + (M_x)_{pe_2} = -M_x = -\int_{-h/2}^{h/2} \sigma_x \left(1 + \frac{z}{R}\right) z dz$$

$$(M_\theta)_{pe_1} + (M_\theta)_{pe_2} = -M_\theta = -\int_{-h/2}^{h/2} \sigma_\theta z dz$$

$$(N_x)_{pe_1} + (N_x)_{pe_2} = -N_x = -\int_{-h/2}^{h/2} \sigma_x \left(1 + \frac{z}{R}\right) dz$$

$$(N_\theta)_{pe_1} + (N_\theta)_{pe_2} = -N_\theta = -\int_{-h/2}^{h/2} \sigma_\theta dz$$

which yields

$$
\begin{aligned}
(M_x)_{pe_1} + (M_x)_{pe_2} &= \frac{-Eh^3}{12(1-\nu^2)}\left[\kappa_x + \nu\kappa_\theta + \frac{\varepsilon_x}{R}\right] \\
(M_\theta)_{pe_1} + (M_\theta)_{pe_2} &\approx \frac{-Eh^3}{12(1-\nu^2)}\left[\kappa_\theta + \nu\kappa_x - \frac{\varepsilon_\theta}{R}\right] \\
(N_x)_{pe_1} + (N_x)_{pe_2} &= \frac{-Eh}{1-\nu^2}\left[\varepsilon_x + \nu\varepsilon_\theta + \frac{h^2}{12}\frac{\kappa_x}{R}\right] \\
(N_\theta)_{pe_1} + (N_\theta)_{pe_2} &\approx \frac{-Eh}{1-\nu^2}\left[\varepsilon_\theta + \nu\varepsilon_x + \frac{h^2}{12}\frac{\kappa_\theta}{R}\right]
\end{aligned}
\tag{3.12}
$$

The two tangential expressions are approximate in the sense that the terms $(1 + z/R)^{-1}$ are replaced by the truncated geometric series $1 - z/R$ before integration (this is the same strategy which is used when determining the moment and force resultants in the Byrne-Flügge-Lur'ye general shell theory). The patch resultants in (3.12) are then used in (3.9) to determine the total line forces and moments generated by the finite patches. Because these resultants are functions of the material properties as well as the midsurface characteristics, they can be easily constructed once $\varepsilon_x, \varepsilon_\theta, \kappa_x$ and κ_θ have been determined. This is again accomplished by moment and force balancing.

Determination of the Midsurface Characteristics

In terms of the stresses, the moment and force equilibrium equations (3.10) and (3.11) can be written as

$$
\begin{aligned}
\int_{-h/2}^{h/2} \sigma_x \left(1 + \frac{z}{R}\right) z dz + \int_{h/2}^{h/2+T} (\sigma_x)_{pe_1} \left(1 + \frac{z}{R}\right) z dz + \int_{-h/2-T}^{-h/2} (\sigma_x)_{pe_2} \left(1 + \frac{z}{R}\right) z dz = 0 \\
\int_{-h/2}^{h/2} \sigma_\theta z dz + \int_{h/2}^{h/2+T} (\sigma_\theta)_{pe_1} z dz + \int_{-h/2-T}^{-h/2} (\sigma_\theta)_{pe_2} z dz = 0
\end{aligned}
\tag{3.13}
$$

and

$$
\begin{aligned}
\int_{-h/2}^{h/2} \sigma_x \left(1 + \frac{z}{R}\right) dz + \int_{h/2}^{h/2+T} (\sigma_x)_{pe_1} \left(1 + \frac{z}{R}\right) dz + \int_{-h/2-T}^{-h/2} (\sigma_x)_{pe_2} \left(1 + \frac{z}{R}\right) dz = 0 \\
\int_{-h/2}^{h/2} \sigma_\theta dz + \int_{h/2}^{h/2+T} (\sigma_\theta)_{pe_1} dz + \int_{-h/2-T}^{-h/2} (\sigma_\theta)_{pe_2} dz = 0 \, .
\end{aligned}
\tag{3.14}
$$

The integrals appearing in (3.13) and (3.14) are explicitly evaluated in the [1].

After collecting terms, this yields the 4×4 linear system

$$
[A_{shell} + A_1 + A_2]\, e = e_{pe_1} f_1 + e_{pe_2} f_2 \tag{3.15}
$$

in the unknowns $e = (\varepsilon_x, \varepsilon_\theta, \kappa_x, \kappa_\theta)^T$. The shell contributions in A_{shell}, the outer patch contributions in A_1 and f_1, and the inner patch terms in A_2 and f_2 are

$$A_{shell} = \begin{bmatrix} \frac{E_1}{R} & 0 & E_1 & E_1\nu \\ 0 & -\frac{E_1}{R} & E_1\nu & E_1 \\ E_2 & E_2\nu & \frac{1}{R}\frac{E_2h^2}{12} & 0 \\ E_2\nu & E_2 & 0 & -\frac{1}{R}\frac{E_2h^2}{12} \end{bmatrix}$$

$$A_1 = \begin{bmatrix} \frac{a_2}{R} + a_3 & a_3\nu_{pe} & \frac{a_1}{R} + a_2 & a_2\nu_{pe} \\ a_3\nu_{pe} & -\frac{a_2}{R} + a_3 & a_2\nu_{pe} & \frac{a_1}{R} + a_2 \\ \frac{a_3}{R} + T & T\nu_{pe} & \frac{a_4}{R} + a_3 & a_3\nu_{pe} \\ T\nu_{pe} & -\frac{a_3}{R} + T & a_3\nu_{pe} & -\frac{a_4}{R} + a_3 \end{bmatrix}$$

$$A_2 = \begin{bmatrix} \frac{a_2}{R} - a_3 & -a_3\nu_{pe} & -\frac{a_1}{R} + a_2 & a_2\nu_{pe} \\ -a_3\nu_{pe} & -\frac{a_2}{R} - a_3 & a_2\nu_{pe} & -\frac{a_1}{R} + a_2 \\ -\frac{a_3}{R} + T & T\nu_{pe} & \frac{a_4}{R} - a_3 & -a_3\nu_{pe} \\ T\nu_{pe} & \frac{a_3}{R} + T & -a_3\nu_{pe} & -\frac{a_4}{R} - a_3 \end{bmatrix}$$

and

$$f_1 = (1+\nu_{pe}) \begin{bmatrix} \frac{a_2}{R} + a_3 \\ a_3 \\ \frac{a_3}{R} + T \\ T \end{bmatrix} \quad , \quad f_2 = (1+\nu_{pe}) \begin{bmatrix} \frac{a_2}{R} - a_3 \\ -a_3 \\ -\frac{a_3}{R} + T \\ T \end{bmatrix}$$

with

$$E_1 = \frac{Eh^3(1-\nu_{pe}^2)}{12E_{pe}(1-\nu^2)} \quad , \quad E_2 = \frac{Eh(1-\nu_{pe}^2)}{E_{pe}(1-\nu^2)}$$

$$a_1 = \frac{1}{64}\left[16\left(\frac{h}{2}+T\right)^4 - h^4\right] \quad , \quad a_3 = \frac{1}{8}\left[4\left(\frac{h}{2}+T\right)^2 - h^2\right]$$

$$a_2 = \frac{1}{24}\left[8\left(\frac{h}{2}+T\right)^3 - h^3\right] \quad , \quad a_4 = \frac{T}{12}\left[3h^2 + 6hT + 4T^2\right] .$$

Note that the coefficients a_i , $i = 1, \cdots, 4$, are of order at most three in h.

We point out that A_{shell}, A_1, A_2, f_1 and f_2 depend on material properties of the patches and shell (thickness, elastic properties, and Poisson ratios), the radius of curvature of the shell, and the voltage being applied to the patches (recall that $e_{pe_1} = d_{31}V_1/T$ where V_1 is the applied voltage into the outer patch with a similar definition for e_{pe_2}). The above formulation isolates the contributions due to the individual patches and is useful if one wants to activate only one of the patches. If both patches are present, the above formulation can be simplified to yield the linear system

$$Ae = e_{pe_1} f_1 + e_{pe_2} f_2$$

where

$$A = \begin{bmatrix} \frac{1}{R}(E_1 + 2a_2) & 0 & E_1 + 2a_2 & E_1\nu + 2a_2\nu_{pe} \\ 0 & -\frac{1}{R}(E_1 + 2a_2) & E_1\nu + 2a_2\nu_{pe} & E_1 + 2a_2 \\ E_2 + 2T & E_2\nu + 2T\nu_{pe} & \frac{1}{R}\left(\frac{E_2h^2}{12} + 2a_4\right) & 0 \\ E_2\nu + 2T\nu_{pe} & E_2 + 2T & 0 & -\frac{1}{R}\left(\frac{E_2h^2}{12} + 2a_4\right) \end{bmatrix}.$$

Algorithm for Determining the Shell/Patch Interactions

The steps which are necessary for solving for the shell loads due to the activation of the patches can be summarized as follows.

(1) Set up the 4×4 system $Ae = f$ and solve for $e = (\varepsilon_x, \varepsilon_\theta, \kappa_x, \kappa_\theta)^T$ which contains the midsurface strains and changes in curvature.

(2) Determine the line moments and forces which are generated by the individual patches as set up in (3.12).

(3) The corresponding combined resultants for finite patches are given by (3.9).

(4) The resultants from (3.9) are directly substituted into (2.13) as the load on the shell if the weak shell equations are being used (recall that in this case, $\hat{q}_n = 0$ and $\hat{N}_x = (N_x)_{pe}$, $\hat{N}_\theta = (N_\theta)_{pe}$, $\hat{M}_x = (M_x)_{pe}$, $\hat{M}_\theta = (M_\theta)_{pe}$ as summarized in (3.1)). For the strong form of the equations of motion, the derivative expressions in (3.2) are formed and substituted into (2.8) as the external load.

We point out that the substitution of the patch moments and forces into the strong form of the shell equations results in one derivative of the Heaviside and indicator functions for the forces and two derivatives of the Heaviside function for the moments whereas no such differentiation is required in the weak form (the derivatives are transferred onto the test functions and one simply integrates over the region covered by the patches). This is one motivation for using the weak form of the shell equations in many applications.

4 Patch Contributions to Plate and Beam Equations

Analysis similar to that used for the thin cylindrical shells can be used to determine the forces and moments which are due to the activation of piezoceramic patches which have been bonded to a flat plate or beam.

Plate/Patch Interactions

The patch interactions with a flat plate can be determined in a manner similar to that used in the study of the interactions between a thin cylindrical shell and a pair of piezoceramic patches as discussed in the last section. Direct force and moment balancing leads to the 4×4 system listed under Method 1, and this system can then be solved for the unknowns $\varepsilon_x, \varepsilon_y, \kappa_x$ and κ_y. By then substituting these values into resultant expressions similar to those in (3.12), one obtains the forces and moments generated by the patch. This procedure can be simplified however, by noting that the strains in the x and y directions of a homogeneous flat plate are equal when equal free strains are generated by the patch (see [6]). Hence two of the variables can be eliminated which leads to the more easily solved 2×2 system given under Method 2. It should be noted that the two methods yield the same final force and moment resultants.

Method 1

Force and moment balancing similar to that used in the study of the patch/shell interactions yields the system

$$[A_{plate} + A_1 + A_2]\, e = e_{pe_1} f_1 + e_{pe_2} f_2$$

where $e = (\varepsilon_x, \varepsilon_y, \kappa_x, \kappa_y)^T$. The matrices and vectors containing contributions due to the plate and two patches are

$$A_{plate} = \begin{bmatrix} 0 & 0 & E_1 & E_1\nu \\ 0 & 0 & E_1\nu & E_1 \\ E_2 & E_2\nu & 0 & 0 \\ E_2\nu & E_2 & 0 & 0 \end{bmatrix}$$

$$A_1 = \begin{bmatrix} a_3 & a_3\nu_{pe} & a_2 & a_2\nu_{pe} \\ a_3\nu_{pe} & a_3 & a_2\nu_{pe} & a_2 \\ T & T\nu_{pe} & a_3 & a_3\nu_{pe} \\ T\nu_{pe} & T & a_3\nu_{pe} & a_3 \end{bmatrix}, \quad A_2 = \begin{bmatrix} -a_3 & -a_3\nu_{pe} & a_2 & a_2\nu_{pe} \\ -a_3\nu_{pe} & -a_3 & a_2\nu_{pe} & a_2 \\ T & T\nu_{pe} & -a_3 & -a_3\nu_{pe} \\ T\nu_{pe} & T & -a_3\nu_{pe} & -a_3 \end{bmatrix}$$

and

$$f_1 = (1+\nu_{pe}) \begin{bmatrix} a_3 \\ a_3 \\ T \\ T \end{bmatrix}, \quad f_2 = (1+\nu_{pe}) \begin{bmatrix} -a_3 \\ -a_3 \\ T \\ T \end{bmatrix}$$

with

$$E_1 = \frac{Eh^3(1-\nu_{pe}^2)}{12E_{pe}(1-\nu^2)} \quad , \quad E_2 = \frac{Eh(1-\nu_{pe}^2)}{E_{pe}(1-\nu^2)}$$

$$a_2 = \frac{1}{24}\left[8\left(\frac{h}{2}+T\right)^3 - h^3\right] \quad , \quad a_3 = \frac{1}{8}\left[4\left(\frac{h}{2}+T\right)^2 - h^2\right] .$$

Note that these matrices and vectors are identical to those of (3.15) if one takes $R \to \infty$ in the latter expressions. Once $\varepsilon_x, \varepsilon_y, \kappa_x$ and κ_y have been determined, the moment and force resultants can be found in a manner similar to that used for shells.

Method 2

Here we take advantage of the fact that for a homogeneous plate, the strains in the x and y directions will be equal when generated by equal free (unconstrained) strains from the patch. Hence we take

$$e = e_x = e_y = \varepsilon + \kappa z$$

as the strain distribution in both the plate and the patch. This yields the stresses

$$\sigma = \sigma_x = \sigma_y = \frac{E}{1-\nu} e$$

in the plate and

$$(\sigma)_{pe_1} = (\sigma_x)_{pe_1} = (\sigma_y)_{pe_1} = \frac{E_{pe}}{1-\nu_{pe}}(e - e_{pe_1})$$

$$(\sigma)_{pe_2} = (\sigma_x)_{pe_2} = (\sigma_y)_{pe_2} = \frac{E_{pe}}{1-\nu_{pe}}(e - e_{pe_2})$$

in the patch. The force and moment resultants for the patches can be found either by integrating the stresses over the patches or by using force and moment balancing to express them in terms of the resultants for the forced plate. As was done in the shell analysis, we will take the latter approach since it yields simpler expressions for the external resultants. Force and moment balancing in conjunction with integration of the forced plate resultants then yields

$$\begin{aligned} (M_x)_{pe_1} + (M_x)_{pe_2} &= (M_y)_{pe_1} + (M_y)_{pe_2} = \frac{-Eh^3}{12(1-\nu)}\kappa \\ (N_x)_{pe_1} + (N_x)_{pe_2} &= (N_y)_{pe_1} + (N_y)_{pe_2} = \frac{-Eh}{1-\nu}\varepsilon \ . \end{aligned} \tag{4.1}$$

As expected, these relations agree with those in (3.12) for the forced shell with the exception of the $\mathcal{O}(1/R)$ terms in the latter case which are due to the curvature.

The total resultants generated by a pair of patches with edges parallel to lines of constant x and y can be determined in a manner similar to that used with the shells. For a patch with bounding values x_1, x_2, y_1 and y_2, the total resultants are

$$\begin{aligned} (M_x)_{pe} &= (M_y)_{pe} = [(M_x)_{pe_1} + (M_x)_{pe_2}]\,[H_1(x) - H_2(x)]\,[H_1(y) - H_2(y)] \\ (N_x)_{pe} &= (N_y)_{pe} = [(N_x)_{pe_1} + (N_x)_{pe_2}]\,[H_1(x) - H_2(x)]\,[H_1(y) - H_2(y)]\,S_{1,2}(x)\tilde{S}_{1,2}(y) \end{aligned} \tag{4.2}$$

where again, $H_i(x) \equiv H(x - x_i)$, $i = 1, 2$, $S_{1,2}(x)$ denotes the indicator function described in (3.3), and $H_i(y)$ and $\tilde{S}_{1,2}(y)$ are defined in an analogous manner.

As before, ε and κ must be found in order to determine the resultants in (4.2). This is accomplished via moment and force balancing which then yields the system

$$[A_{plate} + A_1 + A_2]\, e = e_{pe_1} f_1 + e_{pe_2} f_2 \tag{4.3}$$

where $e = (\varepsilon, \kappa)^T$. The component matrices and vectors are

$$A_{plate} = \begin{bmatrix} 0 & E_1 \\ E_2 & 0 \end{bmatrix} \quad , \quad A_1 = \begin{bmatrix} a_3 & a_2 \\ T & a_3 \end{bmatrix} \quad , \quad A_2 = \begin{bmatrix} -a_3 & a_2 \\ T & -a_3 \end{bmatrix}$$

and

$$f_1 = \begin{bmatrix} a_3 \\ T \end{bmatrix} \quad , \quad f_2 = \begin{bmatrix} -a_3 \\ T \end{bmatrix} .$$

The subscripts 1 and 2 again refer to the outer and inner patch contributions, respectively, and the constants E_1, E_2, a_2 and a_3 are given by

$$E_1 = \frac{Eh^3(1 - \nu_{pe})}{12E_{pe}(1 - \nu)} \quad , \quad E_2 = \frac{Eh(1 - \nu_{pe})}{E_{pe}(1 - \nu)}$$

$$a_2 = \frac{1}{24}\left[8\left(\frac{h}{2} + T\right)^3 - h^3\right] = \frac{1}{4}h^2T + \frac{1}{2}hT^2 + \frac{1}{3}T^3$$

$$a_3 = \frac{1}{8}\left[4\left(\frac{h}{2} + T\right)^2 - h^2\right] = \frac{1}{2}T(h + T) .$$

Algorithm for Determining the Plate/Patch Interactions

As in the case of the shell, the steps necessary for determining the plate loads which are due to the patches can be summarized in a simple algorithm.

(1) Set up and solve the 2×2 system $Ae = f$ in (4.3) where $e = (\varepsilon, \kappa)^T$ contains the midsurface strain and change in curvature.

(2) Determine the combined resultants for the finite patches through (4.2) in conjunction with (4.1).

(3) Once determined, the resultants from (4.2) can be substituted directly into the weak form of the plate equations (2.15) as the load on the system (with $\hat{q}_n = 0$ and $\hat{N}_x = (N_x)_{pe}$, $\hat{N}_y = (N_y)_{pe}$, $\hat{M}_x = (M_x)_{pe}$, $\hat{M}_y = (M_y)_{pe}$). If the strong form of the plate equations is being used, the surface loads can be determined via the expressions

$$\hat{q}_x = -S_{1,2}(x)\tilde{S}_{1,2}(y)\frac{\partial (N_x)_{pe}}{\partial x} \quad , \quad \hat{q}_y = -S_{1,2}(x)\tilde{S}_{1,2}(y)\frac{\partial (N_y)_{pe}}{\partial y}$$

$$\hat{m}_x = -\frac{\partial (M_y)_{pe}}{\partial y} \quad , \quad \hat{m}_y = -\frac{\partial (M_x)_{pe}}{\partial x} ,$$

and these latter values can be substituted into the equilibrium equations (2.14).

As in the case of the shells, the use of the strong form results in up to two derivatives of the Heaviside function whereas the use of the weak form alleviates this problem by transferring the derivatives onto the test functions.

It should be noted that the voltage choice $e_{pe} = e_{pe_1} = e_{pe_2}$ causes pure extension (patch pairs excited "in phase") in the plate while pure bending occurs with the choice $e_{pe} = -e_{pe_1} = e_{pe_2}$ ("out of phase" excitation).

Special Case: $e_{pe} = -e_{pe_1} = e_{pe_2}$

In this case, the constants ε and κ have the values

$$\varepsilon = 0 \quad , \quad \kappa = -\frac{2a_3}{E_1 + 2a_2} e_{pe}$$

which leads to the total patch moments

$$(M_x)_{pe} = (M_y)_{pe} = \frac{Th(h+T)}{h^3 + \beta\,(6h^2T + 12hT^2 + 8T^3)} h^2 \gamma e_{pe} \left[H_1(x) - H_2(x)\right] \left[H_1(y) - H_2(y)\right]$$

where

$$\beta = \frac{E_{pe}(1-\nu)}{E(1-\nu_{pe})} \quad , \quad \gamma = \frac{E_{pe}}{(1-\nu_{pe})} \, .$$

This line moment expression is equivalent to the relation

$$M_x = M_y = \frac{\rho_z(2+\rho_z)}{1 + \beta\rho_z(3 + \rho_z^2 + 3\rho_z)} h^2 \gamma e_{pe} \left[H_1(x) - H_2(x)\right] \left[H_1(y) - H_2(y)\right]$$

with $\rho_z = T/\hat{h}, \hat{h} = h/2$ which was obtained by Kim and Jones [12] in their development of a model for the bending interactions between a flat plate and a piezoelectic actuator. In their work, they consider a patch configuration which excites pure bending in the plate and then determine the effective patch moment by first isolating the interface stress of the system.

Beam/Patch Interactions

The patch contributions to the dynamics of a thin beam can be determined directly from the plate/patch interaction model if one considers only vibrations in the x-direction along with the usual transverse vibrations. The system for the beam/patch configuration is then identical to that found in (4.3) with the constants E_1 and E_2 now given by

$$E_1 = \frac{h^3}{12} \frac{E}{E_{pe}} \quad , \quad E_2 = h \frac{E}{E_{pe}} \, .$$

Once ε and κ have been determined, the force and moment resultants for the patch are expressed in terms of those of the forced beam and are given by

$$\begin{aligned} (M_x)_{pe_1} + (M_x)_{pe_2} &= -EI\kappa \\ (N_x)_{pe_1} + (N_x)_{pe_2} &= -Eh\varepsilon \end{aligned} \tag{4.4}$$

where $I = h^3/12$ is the moment of inertia for the beam. For patches with bounding values x_1 and x_2, the effective moments and forces are

$$(M_x)_{pe} = [(M_x)_{pe_1} + (M_x)_{pe_2}]\,[H(x - x_1) - H(x - x_2)]$$
$$(N_x)_{pe} = [(N_x)_{pe_1} + (N_x)_{pe_2}]\,[H(x - x_1) - H(x - x_2)]\,S_{1,2}(x)$$

which can then be substituted directly into the weak equations (2.18) as loads on the beam (with $\hat{q}_n = 0$ and $\hat{N}_x = (N_x)_{pe}, \hat{M}_x = (M_x)_{pe}$). In order to determine the patch loads for the strong form of the beam equations, the corresponding surface moments and forces are found via the relationships

$$(q_x)_{pe} = -S_{1,2}(x)\frac{\partial (N_x)_{pe}}{\partial x} \quad , \quad (m_y)_{pe} = -\frac{\partial (M_x)_{pe}}{\partial x}$$

and these latter values are used in (2.17). We again point out that this results in the need to differentiate the Heaviside function (once for the force and twice for the moment) whereas this problem is avoided in the weak formulation since the derivatives are transferred onto the test functions. In fact, the effect of the Heaviside functions in the latter case is to simply restrict the integrals to the region covered by the patches.

Special Case: Top Patch Activation

Consider the problem of a beam having only a top activating patch. The system in this case is

$$\begin{bmatrix} a_3 & E_1 + a_2 \\ E_2 + T & a_3 \end{bmatrix} \begin{bmatrix} \varepsilon \\ \kappa \end{bmatrix} = e_{pe} \begin{bmatrix} a_3 \\ T \end{bmatrix}$$

which implies that the midsurface constants are then given by

$$\varepsilon = \frac{E_{pe}T\,(E_{pe}T^3 + Eh^3)}{E_{pe}^2T^4 + 4EE_{pe}T^3h + 6EE_{pe}T^2h^2 + 4EE_{pe}Th^3 + E^2h^4} \cdot e_{pe_1}$$

$$\kappa = \frac{6EE_{pe}Th(T + h)}{E_{pe}^2T^4 + 4EE_{pe}T^3h + 6EE_{pe}T^2h^2 + 4EE_{pe}Th^3 + E^2h^4} \cdot e_{pe_1} \ .$$

These expressions for ε and κ are the same as those found by Gibbs and Fuller [10] when they were investigating the moments and forces generated by a single patch which was bonded to a thin beam (these expressions are equivalent to their (7) and (8) once the latter have been simplified and $h/2$ has been substituted for h). The moment and force resultants $(M_x)_{pe_1}$ and $(N_x)_{pe_1}$ can then be found by substituting ε and κ into (4.4) (with $(M_x)_{pe_2} = (N_x)_{pe_2} = 0$ since there is no bottom patch). We note that the resultants in this case are equivalent to those in [10] although the forms and signs differ slightly due to a slight difference in the formulation of the underlying beam equations.

5 Conclusion

In this work, general models describing the interactions between a pair of piezoceramic patches and an underlying elastic structure have been presented. While the presentation is for elastic substructures consisting of a thin cylindrical shell, plate and beam, the techniques discussed for determining the moments and forces generated by the patches can be directly extended to more complex structures and geometries.

In the case of the shell, the patches are assumed to be curved and the coupling between the in-plane strains and the bending, which is due to the curvature, is retained. By using force and moment balancing to determine the midsurface strains and changes in curvature of the combined structure, expressions for the patch moment and force resultants can be developed. In this manner, the loading due to an actuating pair of patches can be expressed in terms of the material properties of the shell and patches (thickness, elastic properties and Poisson ratios), the radius of curvature of the shell, and the voltage being applied to each of the patches. This provides a shell/patch interaction model which retains the curvature effects as well as admits potentially different voltages into the two patches. We point out that the general techniques used for determining this cylindrical shell/patch model can also be used to determine the interactions between pairs of piezoceramic patches and more general shells (for example, in the case of a spherical shell, one would retain the curvature effects in both coordinate directions).

The techniques for determining the patch interactions with a cylindrical shell were then used to develop general interaction models for patches which are bonded to thin flat plates and beams. As in the shell case, the models are sufficiently general to allow for potentially differing patch voltages which implies that they can be used for controlling system dynamics when both flexural and extensional vibrations are present. To compare with existing analyses, the plate/patch interaction model is shown to be equivalent to that of [12] in the special case when pure bending motion is excited. Also, the beam/patch model is equivalent to that of [10] when there is one actuating patch. Hence the beam and plate interaction models are consistent with existing theories in the special cases previously examined while also allowing for more general structure/patch interactions which can arise in more complex applications (for example, coupled systems).

For each of the shell, plate and beam interaction models, the contributions of the patches are carefully described in both the strong and weak forms of the time-dependent structural equations of motion. This provides models which can be used in a variety of applications including numerical simulations, parameter identification, and control schemes. In each of these applications, the models are sufficiently general to provide for a variety of approximation techniques including modal, spectral, spline and finite element schemes. Finally, the patch loads determined by these interaction models can be applied to higher order structural models in exactly the same manner, and analogous models can be used for multiple patch pairs and more complex geometries.

ACKNOWLEDGEMENTS: The authors would like to express their sincere appreciation to H.C. Lester and R.J. Silcox of the Acoustics Division, NASA Langley Research Center, for many helpful discussions during various phases of this work.

References

[1] H.T. Banks and R.C. Smith, "Modeling Aspects for Piezoceramic Patch Activation of Shells, Plates and Beams," Center for Research in Scientific Computation Technical Report, CRSC-TR92-12, North Carolina State University, November 1992.

[2] R.L. Clark, Jr., C.R. Fuller and A. Wicks, "Characterization of Multiple Piezoelectric Actuators for Structural Excitation," *Journal of Acoustical Society of America*, to appear, 1992.

[3] E.F. Crawley and E.H. Anderson, "Detailed Models of Piezoceramic Actuation of Beams," AIAA Paper 89-1388-CP, 1989.

[4] E.F. Crawley and J. de Luis, "Use of Piezoelectric Actuators as Elements of Intelligent Structures," AIAA Journal, Vol. 25, No. 10, October, 1987, 1373-1385.

[5] E.F. Crawley, J. de Luis, N.W. Hagood and E.H. Anderson, "Development of Piezoelectric Technology for Applications in Control of Intelligent Structures," Applications in Control of Intelligent Structures, American Controls Conference, Atlanta, June 1988, 1890-1896.

[6] E.K. Dimitriadis, C.R. Fuller and C.A. Rogers, "Piezoelectric Actuators for Distributed Noise and Vibration Excitation of Thin Plates," *Journal of Vibration and Acoustics*, Vol. 13, 1991, 100-107.

[7] C.L. Dym, *Introduction to the Theory of Shells,* Pergamon Press, New York, 1974.

[8] C.R. Fuller, G.P. Gibbs and R.J. Silcox, "Simultaneous Active Control of Flexural and Extensional Power Flow in Beams," *Journal of Intelligent Materials, Systems and Structures*, Vol. 1, No. 2, April 1990.

[9] C.R. Fuller, S.D. Snyder, C.H. Hansen and R.J. Silcox, "Active Control of Interior Noise in Model Aircraft Fuselages Using Piezoceramic Actuators," Paper 90-3922, AIAA 13th Aeroacoustics Conference, Tallahassee, FL, October 1990.

[10] G.P. Gibbs and C.R. Fuller, "Excitation of Thin Beams Using Asymmetric Piezoelectric Actuators," Proceedings of the 121^{st} Meeting of the ASA, Baltimore, MD, April 1991.

[11] J. Jia and C.A. Rogers, "Formulation of a Laminated Shell Theory Incorporating Embedded Distributed Actuators," The American Society of Mechanical Engineers, Reprinted from *AD-Vol. 15, Adaptive Structures*, Editor: B.K. Wada, Book No. H00533, 1989.

[12] S.J. Kim and J.D. Jones, "Optimal Design of Piezo-Actuators for Active Noise and Vibration Control," AIAA 13th Aeroacoustics Conference, Tallahassee, FL, October 1990.

[13] H. Kraus, *Thin Elastic Shells: An Introduction to the Theoretical Foundations and the Analysis of Their Static and Dynamic Behavior,* John Wiley and Sons, Inc., New York, 1967.

[14] A.W. Leissa, *Vibration of Shells*, NASA SP-288, 1973.

[15] H.C. Lester and S. Lefebvre, "Piezoelectric Actuator Models for Active Sound and Vibration Control of Cylinders," Proceedings of the Conference on Recent Advance in Active Control of Sound and Vibration, Blacksburg, VA, 1991, 3-26.

[16] S. Markuš, *The Mechanics of Vibrations of Cylindrical Shells,* Elsevier, New York, 1988.

[17] A.S. Saada, *Elasticity Theory and Applications,* Robert E. Krieger Publishing Company, Malabar, FL, 1987.

[18] S. Timoshenko and S. Woinowsky-Krieger, *Theory of Plates and Shells,* Second Edition, McGraw-Hill Book Company, Inc., New York, 1987.

[19] H.S. Tzou and M. Gadre, "Theoretical Analysis of a Multi-Layered Thin Shell Coupled with Piezoelectric Actuators for Distributed Vibration Controls," *Journal of Sound and Vibration*, 132(3), 1989, 433-450.

REPORT DOCUMENTATION PAGE

Form Approved
OMB No. 0704-0188

Public reporting burden for this collection of information is estimated to average 1 hour per response, including the time for reviewing instructions, searching existing data sources, gathering and maintaining the data needed, and completing and reviewing the collection of information. Send comments regarding this burden estimate or any other aspect of this collection of information, including suggestions for reducing this burden, to Washington Headquarters Services, Directorate for Information Operations and Reports, 1215 Jefferson Davis Highway, Suite 1204, Arlington, VA 22202-4302, and to the Office of Management and Budget, Paperwork Reduction Project (0704-0188), Washington, DC 20503

1. AGENCY USE ONLY (Leave blank)	2. REPORT DATE	3. REPORT TYPE AND DATES COVERED
	December 1992	Contractor Report

4. TITLE AND SUBTITLE
THE MODELING OF PIEZOCERAMIC PATCH INTERACTIONS WITH SHELLS, PLATES AND BEAMS

5. FUNDING NUMBERS
C NAS1-18605
C NAS1-19480

WU 505-90-52-01

6. AUTHOR(S)
H.T. Banks
R.C. Smith

7. PERFORMING ORGANIZATION NAME(S) AND ADDRESS(ES)
Institute for Computer Applications in Science and Engineering
Mail Stop 132C, NASA Langley Research Center
Hampton, VA 23681-0001

8. PERFORMING ORGANIZATION REPORT NUMBER
ICASE Report No. 92-66

9. SPONSORING/MONITORING AGENCY NAME(S) AND ADDRESS(ES)
National Aeronautics and Space Administration
Langley Research Center
Hampton, VA 23681-0001

10. SPONSORING/MONITORING AGENCY REPORT NUMBER
NASA CR-189740
ICASE Report No. 92-66

11. SUPPLEMENTARY NOTES
Langley Technical Monitor: Michael F. Card
Final Report

Submitted to Quarterly of Applied Mathematics

12a. DISTRIBUTION/AVAILABILITY STATEMENT
Unclassified - Unlimited

Subject Category 66

12b. DISTRIBUTION CODE

13. ABSTRACT *(Maximum 200 words)*

General models describing the interactions between a pair of piezoceramic patches and elastic substructures consisting of a cylindrical shell, plate and beam are presented. In each case, the manner in which the patch loads enter both the strong and weak forms of the time-dependent structural equations of motion is described. Through force and moment balancing, these loads are then determined in terms of material properties of the patch and substructure (thickness, elastic properties, Poisson ratios), the geometry of the patch placement, and the voltages into the patches. In the case of the shell, the coupling between bending and inplane deformations, which is due to the curvature, is retained. These models are sufficiently general to allow for potentially different patch voltages which implies that they can be suitably employed when using piezoceramic patches for controlling system dynamics when both extensional and bending vibrations are present.

14. SUBJECT TERMS	15. NUMBER OF PAGES
piezoceramic patches, fully coupled actuator model	33
	16. PRICE CODE A03

17. SECURITY CLASSIFICATION OF REPORT	18. SECURITY CLASSIFICATION OF THIS PAGE	19. SECURITY CLASSIFICATION OF ABSTRACT	20. LIMITATION OF ABSTRACT
Unclassified	Unclassified		